

US Patent & Trademark Office

Patent Public Search | Text View

United States Patent Application Publication

20250259321

Kind Code

A1

Publication Date

August 14, 2025

Inventor(s)

ANTSFELD; Leonid et al.

TRAINING OF MODELS FOR MONOCULAR DEPTH AND VISUAL ODOMETRY

Abstract

A non-transitory computer readable medium storing a computer model is described, where the model includes: an encoder module configured to encode first and second images into first and second representations, respectively, the first and second images being from consecutive frames from video; a first decoder module configured to decode the first and second representations and generate first and second depth maps for the images based on the first and second representations, respectively; and a second decoder module configured to determine a six degree of freedom pose translation of a camera that captured the video based on the first and second representations.

Inventors: ANTSFELD; Leonid (Saint Ismier, FR), Chidlovskii; Boris (Meylan, FR)

Applicant: NAVER CORPORAION (Gyeonggi-do, KR); NAVER LABS CORPORATION (Gyeonggi-do, KR)

Family ID: 1000007694275

Assignee: NAVER CORPORATION (Gyeonggi-do, KR); NAVER LABS CORPORATION (Gyeonggi-do, KR)

Appl. No.: 18/440243

Filed: February 13, 2024

Publication Classification

Int. Cl.: G06T7/55 (20170101); G06T3/18 (20240101)

U.S. Cl.:

CPC G06T7/55 (20170101); G06T3/18 (20240101); G06T2207/20081 (20130101); G06T2207/20084 (20130101)

Background/Summary

FIELD

[0001] The present disclosure relates to depth and visual odometry and more particularly to systems and methods for training models configured to determine depth and visual odometry.

BACKGROUND

[0002] The background description provided here is for the purpose of generally presenting the context of the disclosure. Work of the presently named inventors, to the extent it is described in this background section, as well as aspects of the description that may not otherwise qualify as prior art at the time of filing, are neither expressly nor impliedly admitted as prior art against the present disclosure.

[0003] Human vision is based on two optical sensors (the eyes) and a highly specialized and effective image analysis engine (the vision related parts of the brain). The image analysis performed by the human brain on the images detected by the eyes allows a human to recognize objects and object edges in images, estimate object distances, and estimate object velocities and future object positions.

[0004] These image analysis capabilities are of importance in everyday human activities such as driving a car, operating machines, catching and throwing objects, hitting a nail with a hammer, navigating through a crowd of people, etc.

[0005] Computer-based devices may be configured to perform human activities autonomously. One element for achieving this goal is to provide computer-based devices with computer vision, an emulation of human vision.

[0006] Similar to the human visual system, a computer vision system may be configured to perform image analysis. A computer vision system may provide a sufficient approximation of the image analysis capabilities of the human brain to allow computer-based devices to perform high-level vision-related tasks such as object and edge recognition, monocular or binocular depth estimation, optical flow estimation, or pose estimation. Some high-level vision-related tasks, such as depth estimation, optical flow estimation or pose estimation, are based on an understanding of the three dimensional (3D) geometry of a depicted scene.

[0007] In the following, this kind of high-level vision-related tasks is summarized in the term geometric vision tasks. Computer vision related technology may be used, for example, in self-driving (autonomous) vehicles, autonomous robotic machines, and other devices. However, enhancements in the computer-based performance of geometric vision tasks may also have great impact in other technical fields such as image based diagnostic or image based material testing.

[0008] Artificial intelligence (AI) based image analysis may be used in computer vision. In AI-based image analysis, a trained machine learning model is applied to one or more images to extract relevant analytic data for a specific geometric vision task from the one or more images (e.g., a depth map, pairs of corresponding pixels, object velocities, etc.). The quality of the extracted analytic data may depend on the training of the machine learning model.

[0009] Typically, a machine learning model includes a large number of learnable parameters. A goal of training the machine learning model is to find a set of parameters, which optimizes the outcome for a specific task on a set of training data. A deviation from an optimum outcome may be expressed as a loss (e.g., the value of a loss function). Finding an optimal set of parameters translates to finding a set of parameters that lead to a minimum value of the loss function. Since the training is based on the deviation of an achieved result to an optimal result for a given task to minimize the loss, the AI system may receive some indication of the optimal result in order to improve during the training phase.

[0010] Supervised training approaches involve annotated training data, which may include ground

truth data indicating the optimum outcome for a specific task. Since annotating the training data may be a significant effort, the amount of available annotated data for a specific task is limited. The problem of limited training data can be alleviated by unsupervised training approaches.

[0011] Unsupervised training may use unannotated training data without explicitly specified ground truth data and can therefore take advantage of large data repositories of unannotated training data (e.g., image databases or internet text repositories). However, unsupervised training may be limited to tasks for which the optimal result of the task can be determined without explicit annotation of ground-truth data.

[0012] Even if the task for which a machine learning model is to be trained does not support unsupervised training, combining unsupervised training and supervised training can provide an enhanced training result. Unsupervised pre-training may be used for various high-level tasks in computer vision. In a second training step, the pre-trained machine learning models (which may be referred to as foundation models) can be fine-tune trained on small annotated datasets and perform well on some tasks compared to supervised learning approaches, and outperform supervised learning approaches when large annotated datasets are not available.

[0013] Unsupervised learning may perform well in a number of high-level computer vision tasks, such as image classification or object detection. These models enable the use of additional image data without requiring additional labels. One example of unsupervised learning involves contrastive learning, which constructs a pretext task by learning model outputs that are invariant to data augmentations. Masked Image Modeling (MIM) may be an alternative for unsupervised learning. These models may be trained using an auto-completion pretext task: an encoder encodes a partial view of an image input, obtained by splitting it into patches and masking some of them, into a latent representation. The invisible patches may then be predicted by the decoder based on the latent representation. These methods are examples of so-called self-supervised learning, which is a specific approach to unsupervised learning. The tasks on which these existing self-supervised methods excel may include single-view semantic oriented tasks, such as image classification or semantic segmentation. However, 3D tasks (e.g., geometric vision tasks) where the 3D geometry of the depicted scene becomes relevant may be difficult to handle.

SUMMARY

[0014] In a feature, a non-transitory computer readable medium storing a computer model is described, where the model includes: an encoder module configured to encode first and second images into first and second representations, respectively, the first and second images being from consecutive frames from video; a first decoder module configured to decode the first and second representations and generate first and second depth maps for the images based on the first and second representations, respectively; and a second decoder module configured to determine a six degree of freedom pose translation of a camera that captured the video based on the first and second representations.

[0015] In further features, the first and second decoder modules include dense prediction transformer (DPT) decoders.

[0016] In further features, the encoder module includes adapter modules trained based on minimizing a geometric consistency loss.

[0017] In further features, the encoder module includes adapter modules trained based on minimizing a photometric loss.

[0018] In further features, the encoder module includes adapter modules trained based on minimizing an edge smoothness loss.

[0019] In a feature, a system includes: a model including: an encoder module configured to encode first and second images into first and second representations, respectively; a first decoder module configured to decode the first and second representations and generate first and second depth maps for the images based on the first and second representations, respectively; and a second decoder module configured to determine a six degree of freedom pose translation of a camera that captured

the video based on the first and second representations; and a training module configured to: train the model using pairs of images, each pair of images including at least part of a same scene and captured at different times; and train parameters of adapter modules of the encoder module using consecutive frames of monocular video based on depth maps and pose translations determined by the model based on the consecutive frames of monocular video.

[0020] In further features, the training module is configured to train the parameters of the adapter modules after training the model using the pairs of images.

[0021] In further features, the training module is configured to train the parameters of the adapter modules without annotations for the frames of the monocular video.

[0022] In further features, the adapter modules include an up projection module, a rectified linear unit (ReLU), and a down projection module, and where the training module is configured to train parameters of at least one of the up projection module, the ReLU, and the down projection module based on the depth maps and pose translations determined by the model based on the consecutive frames of monocular video.

[0023] In further features, the training module is configured to train the parameters of the adapter modules while all other parameters of the model are fixed.

[0024] In further features, the training module is configured to train the parameters of the adapter modules based on minimizing a geometric consistency loss.

[0025] In further features: a warping module is configured to generate a warped depth map based on the first depth map; and a loss module is configured to determine the geometric consistency loss based on differences between the warped depth map and the first depth map.

[0026] In further features, the warping module is configured to generate the warped depth map further based on the pose translation.

[0027] In further features, the warping module is configured to generate the warped depth map based on transforming the first depth map to a three dimensional space and projecting to the second image using the pose translation.

[0028] In further features, the training module is configured to train the parameters of the adapter modules based on minimizing a photometric loss.

[0029] In further features: a warping module is configured to generate a warped image based on the first image; and a loss module is configured to determine the photometric consistency loss based on differences between the warped image and the first image.

[0030] In further features, the loss module is configured to determine the photometric consistency loss based on downweighting regions of the first image including moving objects.

[0031] In further features, the training module is configured to train the parameters of the adapter modules based on minimizing an edge smoothness loss.

[0032] In further features, a loss module is configured to determine the edge smoothness loss based on first derivatives of pixel values of the first and second depth maps.

[0033] In further features, the first and second decoder modules include dense prediction transformer (DPT) decoders.

[0034] In a feature, a method includes: train a model using pairs of images, each pair of images including at least part of a same scene and captured at different times, the model including: an encoder module configured to encode first and second images into first and second representations, respectively; a first decoder module configured to decode the first and second representations and generate first and second depth maps for the images based on the first and second representations, respectively; and a second decoder module configured to determine a six degree of freedom pose translation of a camera that captured the video based on the first and second representations; and training parameters of adapter modules of the encoder module using consecutive frames of monocular video based on depth maps and pose translations determined by the model based on the consecutive frames of monocular video.

[0035] Further areas of applicability of the present disclosure will become apparent from the

detailed description, the claims and the drawings. The detailed description and specific examples are intended for purposes of illustration only and are not intended to limit the scope of the disclosure.

Description

BRIEF DESCRIPTION OF THE DRAWINGS

- [0036] The patent or application file contains at least one drawing executed in color. Copies of this patent or patent application publication with color drawing(s) will be provided by the Office upon request and payment of the necessary fee.
- [0037] The present disclosure will become more fully understood from the detailed description and the accompanying drawings, wherein:
- [0038] FIG. 1 illustrates a functional block diagram for an example procedure for training a machine learning model for a geometric vision task;
- [0039] FIG. 2 illustrates a functional block diagram for an example procedure for unsupervised pre-training of a machine learning model on a pretext task using a pair of unannotated images;
- [0040] FIG. 3 illustrates a functional block diagram for an example procedure for self-supervised cross-view completion pre-training of a pretext machine learning model using a pair of unannotated images;
- [0041] FIG. 4 illustrates a functional block diagram for an example procedure for self-supervised cross-view alignment pre-training of a pretext machine learning model using a pair of unannotated images;
- [0042] FIG. 5 is a flowchart illustrating an example method of training a task specific machine learning model on a downstream geometric vision task;
- [0043] FIG. 6 is a flowchart illustrating a method for unsupervised pre-training of a pretext machine learning model on a pretext task;
- [0044] FIG. 7 is a flowchart illustrating a method for self-supervised cross-view completion pre-training of a pretext machine learning model;
- [0045] FIG. 8 is a flowchart illustrating a method for self-supervised cross-view completion pre-training of a pretext machine learning model;
- [0046] FIG. 9 is a flowchart illustrating a method for generating prediction data according to a down-stream geometric vision task combining the self-supervised cross-view completion pre-training of FIG. 7 and the self-supervised cross-view alignment pre-training of FIG. 8;
- [0047] FIG. 10 illustrates an example functional block diagram of an architecture of a system;
- [0048] FIG. 11 includes a functional block diagram of an example implementation of a training system including a model configured to perform depth and visual odometry;
- [0049] FIG. 12 includes a functional block diagram of a training system;
- [0050] FIG. 13 includes a functional block diagram of the model 130;
- [0051] FIG. 14 includes an example functional block diagram of an example implementation one layer of one of the encoders;
- [0052] FIG. 15 includes an example image and depth maps generated based on the image by other methods and a depth map generated by the model as described herein;
- [0053] FIG. 16 includes example maps of ground truth (GT) tracks of paths followed by vehicles (e.g., navigating robots) in blue and predicted paths generated by the model;
- [0054] FIG. 17 includes a flowchart depicting an example method of training the model for concurrent depth estimation and visual odometry; and
- [0055] FIG. 18 includes a flowchart depicting an example method of fine tune training the model for concurrent depth and visual odometry.
- [0056] In the drawings, reference numbers may be reused to identify similar and/or identical

elements.

DETAILED DESCRIPTION

[0057] Described herein are systems, computer-readable media and methods for training a model for monocular depth and visual odometry. For purposes of explanation, numerous examples and specific details are set forth in order to provide a thorough understanding of the described examples. Examples as defined by the claims may include some or all of the features in these examples alone or in combination with other features described below, and may further include modifications and equivalents of the features and concepts described herein. The illustrative embodiments will be described with reference to the drawings, wherein like elements and structures are indicated by like reference numbers.

[0058] FIG. 1 includes a functional block diagram of an example implementation of the herein described two-phase training process performed by a training module 50 for training a machine learning model. The training starts with the training module 50 performing an unsupervised pre-training 110 of a pretext learning model 130 on the pretext task.

[0059] The pretext machine learning model 130 includes a plurality of learnable parameters θ 132. The pre-training process 110 involves the training module 50 iteratively adapting values of the parameters 132 such that the resulting pretext machine learning model 130 achieves continuously better results on the pretext task.

[0060] The pre-training 110 starts with an initial set of parameter values for the parameters θ 132. The initial set of values for the parameters θ 132 may be selected as a common (e.g. predetermined) value for all parameters θ 132, set the initial parameter values at random such that the initial set of parameter values include a random value for each parameter of the plurality of parameters θ 132, or set in another suitable manner.

[0061] During the pre-training 110, the pretext machine learning model 130 receives from the training module 50 a pair of unannotated images including a first image I.sub.1 120 and a second image I.sub.2 122. The first and second images 120 and 122 depict at least partially the same visual content (e.g. a same scene, a same object, a same person, or a same architectural structure) but from different viewpoints or from a similar viewpoint at different times or under different conditions (e.g., lighting, etc.). In this context a viewpoint from which a scene is depicted may refer to a camera position and/or a camera angle relative to the depicted scene from which the image depicting the scene has been taken. The pixel dimensions of the first and second images 120 and 122 may be equal or may differ from each other. The images 120 and 122 do not include annotations with ground-truth data according to the pretext task.

[0062] Based on the pair of the first and second images 120 and 122, the pretext machine learning model 130 generates a reconstructed image I.sub.R 140. The reconstructed image 140 may be a reconstruction of the first or the second image, or a reconstruction of an image, which can be derived from the first and/or second image by applying predetermined transformations to the first image and/or second image. These predetermined transformations may include applying one or more color transformations to one or both of the images such as a transformation to gray scale, applying one or more geometric transformations to one or both of the images, determining a combination of the first and second images such as a pixel-wise difference between the images, etc.

[0063] The pretext machine learning model 130 translates the images 120 and 122 of the image pair into representations of the images (which may be referred to as latent representations) in a mathematical representation space (a latent space). The representations may be, for example, vectors, matrices, etc.

[0064] Depending on the specific pretext task, the pretext machine learning model 130 may perform transformations on the image representations within the representation space eventually resulting in a representation of the reconstructed image 140. Finally, the representation of the reconstructed image 140 is translated back into the image space, thereby generating the reconstructed image 140. Based on the reconstructed image 140 and/or the representation of the

reconstructed image **140**, a pretext loss **142** is determined by the training module **50**, which expresses the quality of the result achieved by the application of the pretext machine learning model **130** to the images of the image pair. The loss may be determined, for example, based on a comparison of the result (the reconstructed image **140** and/or the representation of the reconstructed image **140**) with an expected result for the pair.

[0065] Generally, in machine learning, a loss may denote the value of a loss function (also called a cost function), which is a function that maps an event or values of one or more variables onto a real number representing a cost associated with the event. An aim of the pre-training phase is for the training module **50** to modify the internal, learnable parameters θ **132** of the pretext machine learning model **130** so that they minimize the pretext loss **142** (i.e., the value of the loss function).

[0066] The loss function may be a complicated real valued scalar function depending on each of the learnable parameters θ **132** of the pretext machine learning model **130**. The optimization of the loss function (which converges towards a minimum) is performed by the training module **50** by back-propagation **144** of loss gradients, which are obtained by the training module from partial derivatives of the loss function with respect to the learnable parameters θ **132** of the pretext machine learning model **130**. These loss gradients are back-propagated by the training module **50** to the respective learnable parameters θ **132** in that they are used to modify (or adapt or update) the learnable parameters θ **132** of the pretext machine learning model **130** to produce a lower loss **142** at the next iteration of the pre-training phase.

[0067] At the next iteration, the machine learning model **130** comprising the modified learnable parameters θ **132** generates another reconstructed image **140** based on the same or another image pair using the modified learnable parameters **132** as discussed above. The translation of this pair of images into representations, the transformations within the representation space, and the generation of the reconstructed image **140** is computed using the modified learnable parameters θ **132**. The modified pretext machine learning model **130** is then now better suited to perform the pretext task on an image pair, leading to a lower loss **142** and to a smaller adaptation of the learnable parameters θ **132** at the next back-propagation of the loss gradients until the loss function converges towards a minimum loss **142** and until adaptation of the learnable parameters θ **132** is necessary anymore. Once the loss function has converged to the minimum, the pretext machine learning model **130** has been successfully pre-trained and the pre-training phase may be complete. In alternative embodiments, the iterative pre-training is not performed until full convergence is reached, but is terminated after a predetermined number of iterations.

[0068] The second training phase is a fine-tuning **150** of a task specific machine learning model **170** by the training module **50**. The term fine-tuning in this context may refer to a training, which is performed subsequent to a pre-training phase based on results of the pre-training. In various implementations, the fine-tuning may be performed by the training module **50** supervised or partially supervised. The term supervised may refer to a training based on annotated training data. Annotated training data includes ground-truth data, which include additional information about an optimal/expected result/outcome of the specific task for which the training is performed. Ground-truth data is not used by the trained machine learning model **170**, but is used by the training module **50** to determine the loss **182** for the specific training task based on a result generated by the trained machine learning model **170** given an input.

[0069] Similar to the pretext machine learning model **130**, the task specific machine learning model **170** includes a plurality of learnable parameters θ' **172**. The fine-tuning is performed similar to the pre-training. However, the task for which the task specific machine learning model **170** is trained by the training module **50** is a geometric vision task for which more accurate training involves the use of annotated (ground truth) data. This task may be referred to as a downstream task indicating that the ultimate goal of the training as a whole is to provide a trained machine learning model optimized for performing this task. The pretext task is a precursor task intended to enhance the training of the task specific machine learning model **170** on the downstream geometric vision task.

[0070] The fine-tuning **150** starts with an initial set of parameter values for the parameters θ' **172**. The training module **50** initializes the parameters **172** to the initial set. The training module **50** initializes at least a portion of the parameters θ' **172** with the values of a corresponding portion of the parameters θ **132** of the pre-trained pretext machine learning model **130**. The initial set of values for the remaining portion of the parameters θ' **172** that are not initialized with parameter values of the pre-trained pretext machine learning model **130** may be set by the training module **50**, for example, to a common (e.g. predetermined) value for all the parameters of the remaining portion of the parameters θ' **172**, at random such that the initial set of parameter values includes a random value for each parameter of the remaining portion of the parameters θ' **172**, or in another suitable manner.

[0071] The task specific machine learning model **170** is applied to one or more annotated images from the training module **50**. FIG. **1** depicts two annotated images P.sub.1 **160** and P.sub.2 **162** as an example. Image P.sub.2 **162** is depicted in a dashed line indicating the optional nature of a second input image. Image P.sub.1 **160** includes ground-truth annotations **164** and image P.sub.2 **162** includes ground-truth annotations **166**. In some examples, the two images P.sub.1 **160** and P.sub.2 **162** may be provided as an image pair, where the ground truth annotations are provided for the pair and not individually for each image. In various implementations, only part of the images are annotated and the fine-tuning is performed partially supervised and partially unsupervised. The number of input images depends on the downstream task. Applying the task specific machine learning model **170** to the one or more images results in task specific output data **180**. In other words, the task specific machine learning model **170** generates task specific output data **180** based on the input image(s). Based on the task specific output data **180** and the ground-truth data of the one or more annotated input images, a task specific loss **182** is determined by the training module **50**. The task specific loss **182** expresses the quality of the task specific output data **180** achieved by the application of the task specific machine learning model **170** to the images of the image pair (or the input image(s)).

[0072] As in the pre-training, the task specific loss **182** denotes the value of a loss function. An aim of the fine-tuning phase is to modify the internal, learnable parameters θ' **172** of the task specific machine learning model **170** by the training module **50** so that they minimize the task specific loss **182** (the value of the loss function). The loss function may be a complicated real value scalar function depending on each of the learnable parameters θ' **172** of the task specific machine learning model **170**. The optimization of the loss function (which converges towards a minimum) is performed by back-propagation **184** of the loss gradients, which are obtained by the training module **50** from the partial derivatives of the loss function with respect to the learnable parameters θ' **172** of the task specific machine learning model **170**. These loss gradients are back-propagated to the respective learnable parameters θ' **172** by the training module **50** in that they are used to modify (or adapt or update) the learnable parameters θ' **172** of the task specific machine learning model **170** to produce a lower loss **182** at the next iteration of the fine-tuning phase.

[0073] At the next iteration, the task specific machine learning model **170** including the modified learnable parameters θ' **172** is applied to the same or other annotated images to generate other task specific output data **180**. In other words, the task specific machine learning model **170** generates new task specific output data **180** based on the input images. The modified task specific machine learning model **170** is now better suited to perform the downstream task on the one or more images, leading to a lower loss **182** and to a smaller adaptation of the learnable parameters θ' **172** at the next back-propagation of the loss gradients, until the loss function converges towards a minimum loss **182** and no adaptation of the learnable parameters θ' **172** is necessary anymore. Once the loss function has converged, the task specific machine learning model **170** has been successfully fine-tuned. In various implementations, the iterative fine-tuning is not performed until full convergence is reached, but is terminated by the training module **50** after a predetermined number of iterations.

[0074] FIG. 2 illustrates an example functional block diagram of the model **130** and of the pre-training phase **110** of the training of FIG. 1. The pretext machine learning model **130** includes an encoder (module) **230**, a representation space block (module) **260**, and a decoder (module) **270**. The encoder **230** includes a set of learnable encoder parameters and the decoder **270** includes a set of learnable decoder parameters. Depending on the specific pretext task, the representation space block **260** may also include a set of learnable parameters. Learnable and trainable may be used interchangeably.

[0075] The pretext machine learning model **130** is applied to (receives) a pair of unannotated images including a first image I.sub.1 **120** and a second image I.sub.2 **122**. The first image **120** depicts visual content from a first viewpoint. The second image **122** depicts at least partially the same visual content (e.g. a same scene, a same object, a same person, or a same architectural structure), but differs from the first image either in the viewpoint from which the same visual content is depicted or in other conditions under which the images have been produced, such as lighting conditions, seasonal differences, the depth of field, focal length, etc. The pixel dimensions of the first and second images **120** and **122** may be equal or may differ from each other. The images **120** and **122** do not need to include annotations with ground-truth data according to the pretext task since the pre-training method is performed unsupervised. In some embodiments the pre-training is performed self-supervised. Self-supervised pre-training may refer to a particular example of unsupervised pre-training, where the loss is determined by the training module **50** based on the unannotated input data (e.g. input images) such that no ground-truth annotations are needed to perform the pre-training.

[0076] The encoder **230** of the pretext machine learning model **130** is applied to the first image I.sub.1 **120** to encode the image into a first representation R.sub.1 **240**. The encoder **230** of the pretext machine learning model **130** is additionally applied to the second image I.sub.2 **122** to independently encode the second image **122** into a second representation R.sub.2 **250**. A representation of an image is an element in a mathematical space (e.g. a vector space). A representation may be for example a vector, a set of vectors, a matrix, or a tensor.

[0077] The representation space block **260** receives the two image representations R.sub.1 **240** and R.sub.2 **250**, and transforms one of the representations (e.g., the representation R.sub.1 **240** of the first image I.sub.1 **120**) into a transformed representation **264**. In one example, the first representation R.sub.1 **240** is transformed according to the second representation R.sub.2 **250** such that the transformed representation **264** aligns with the second representation R.sub.2 **250**. In another example, the first representation is transformed by adding learnable elements to the first representation. The transformation of one representation may depend on the other representation or may be independent of the other representation.

[0078] The decoder **270** decodes the transformed representation **264** into a reconstructed image **140**. The reconstructed image **140** may be a reconstruction of the first or the second image, or a reconstruction of an image derivable from the first and/or second image. Optionally, the decoder **270** receives the image representation, which has not been transformed into the transformed representation **264** as additional input for decoding the transformed representation **264** into the reconstructed image **140**. In an example, where the first image representation R.sub.1 **240** has been transformed into the transformed representation **264**, the decoder **270** may receive the second representation R.sub.2 **250** as additional input to decode the transformed representation **264** into the reconstructed image **140**. In any case, the reconstructed image **140** is generated based on both image representations R.sub.1 **240** and R.sub.2 **250** in that the transformation of the first representation R.sub.1 **240** depends on the second representation R.sub.2 **250** and/or the decoding of the transformed representation **264** (when resulting from a transformation of the first representation R.sub.1 **240**) is based on the second representation R.sub.2 **250**.

[0079] Later, a pretext loss **142** is determined by the training module **50** based on the reconstructed image **140**, and back-propagation **144** is performed by the training module to modify the learnable

parameters of the pretext machine learning model **130** based on minimizing the pretext loss. This includes, in particular, the training module **50** modifying the learnable parameters of the decoder **230** and the encoder **270**. In cases where the representation space block **260** includes learnable parameters, these parameters may also be updated by the training module during the back propagation **144**. The determination of the pretext loss **142** may be based on the reconstructed image **140** and, in particular, may be based on a metric, which quantifies a deviation of the reconstructed image **140** from the image it is supposed to reconstruct. In an example, the reconstructed image **140** may be a reconstruction of the first image I.sub.1 **120**; in this example, the pretext loss **142** may be determined by the training module **50** based on a metric quantifying the deviation of the reconstructed image **140** from the first image I.sub.1 **120**. In another example, the reconstructed image **140** may be a reconstruction of the second image I.sub.2 **122**, and the pretext loss **142** may be determined by the training module **50** based on a metric quantifying the deviation of the reconstructed image **140** from the second image I.sub.2 **122**. Additionally or alternatively, the pretext loss **142** may be determined by the training module **50** based on a metric quantifying the difference between the transformed representation **264** and the image representations R.sub.1 **240** or R.sub.2 **250**, which has not been transformed into the transformed representation **264**.

[0080] In the following, two specific pretext tasks for unsupervised pre-training **110** of pretext machine learning model **130** will be presented with reference to FIG. 3 and FIG. 4.

[0081] FIG. 3 illustrates an example pre-training system for the pretext task of cross-view completion. The term cross-view completion pre-training may refer to the pre-training of a pretext machine learning model for the cross-view completion pretext task. Herein, the abbreviation CroCo will be used to refer to cross-view completion.

[0082] FIG. 4 illustrates an example unsupervised pre-training system for the pretext task of cross-view alignment. The term cross-view alignment pre-training may refer to the pre-training of a pretext machine learning model for the cross-view alignment pretext task. Herein, the abbreviation Caiman will be used to refer to cross-view alignment.

[0083] The cross-view completion pre-training system as illustrated in FIG. 3 is an example implementation of unsupervised pre-training **110**. The pretext machine learning model for CroCo pre-training will be subsequently referred to as a CroCo machine learning model. The CroCo machine learning model corresponds to pretext machine learning model **130** as illustrated in FIG. 2. The CroCo machine learning model includes an encoder (module) **330** (corresponding to encoder **230**), a decoder (module) **370** (corresponding to decoder **270**), and a cross-view completion block (module) **360** (corresponding to representation space block **260**).

[0084] The CroCo machine learning model is applied to (receives) a pair of unannotated images including a first image I.sub.1 **310** and a second image I.sub.2 **320**. The two images depict the same visual content (e.g., a same scene, a same object, a same person, or a same architectural structure) from different viewpoints or from a similar viewpoint at different times or under different conditions (e.g., lighting conditions, seasonal conditions, depth of field, focal length, etc.). The pixel dimensions of the two images may be equal or may differ from each other. The images **310** and **320** do not need to include or have associated annotations with ground-truth data according to the CroCo task since the CroCo pre-training method is performed unsupervised.

[0085] A splitting module **300** splits the first image I.sub.1 **310** into a set p.sub.1 of N.sub.1 non-overlapping image patches p.sub.1.sup.i **312**, $p.sub.1 = \{p.sub.1.sup.1, \dots, p.sub.1.sup.N.sub.1\}$. The different patches p.sub.1.sup.i **312** may have a same pixel size or may differ in pixel size. The patches **312** may have predetermined pixel sizes such as 4×4, 8×8, 12×12, 16×16, or 32×32 pixels. However, the patches **312** may have any other suitable pixel size and may not be quadratic, but rectangular (e.g. 4×8 or 16×32 pixels). For simplicity, FIG. 3 shows a relatively small number of 12 patches **312** for image I.sub.1 **310** labeled a to l. However, the image I.sub.1 **310** can be split in any number of patches, such as based on the image pixel size and the patch pixel size.

[0086] In the same way as the first image I.sub.1 **310**, the splitting module **400** splits the second

image I.sub.2 **320** into a set p.sub.2 of N.sub.2 non-overlapping patches p.sub.2.sup.i **322**, p.sub.2={p.sub.2.sup.1, . . . , p.sub.2.sup.N.sub.2}. The pixel sizes of patches **312** of the first image I.sub.1 **310** and of patches **322** of the second image I.sub.2 **320** may be equal or may differ from each other. In one example, both the first image I.sub.1 **310** and the second image I.sub.2 **320** are split into non-overlapping patches **312** and **322** with a size of 16×16 pixels. The number of patches in the set p.sub.1 may be equal to or higher or lower than the number of patches in the set p.sub.2. [0087] A portion of the patches **312** of the set p.sub.1 is masked by a masking module **305** separating the set p.sub.1 in a set p.sub.1={p.sub.1.sup.i|m.sub.i=1} of masked patches **314** (i.e. patches a, c, d, h, i, j, and k identified with etching) and a set {tilde over (p)}.sub.1={p.sub.1.sup.i|m.sub.i=0} of remaining unmasked patches, where m.sub.i=0 denotes that the patch p.sub.1.sup.i is unmasked and m.sub.i=1 denotes that the patch p.sub.1.sup.i is masked. Masking a patch in this context may refer to marking or otherwise identifying the patch as being a masked patch **314**. In various implementations, the pixel content of a masked patch **314** may not altered or deleted such that the pixel content of the masked patch **314** can still be used to determine a CroCo loss (corresponding to the pretext loss **142**). Which ones of the patches to mask may be selected by the masking module **305** such as randomly from the set of patches **312** of image I.sub.1 **310** according to a predetermined ratio of masked patches to the total number of patches N.sub.1. Alternatively, the masked patches **314** may be chosen by the masking module **304** based on a predetermined pattern or another predetermined selection rule. In an example, the ratio of masked patches to the total number of patches for image I.sub.1 **310** is higher than 0.5. For example only, the ratio may be between 0.75 or 0.95. In FIG. 3 the first image I.sub.1 **310** is split into 12 patches, which are similarly labeled as patches **322** of image I.sub.2 **320**. Only the five patches **312** with the labels b, e, f, g and I are unmasked, the remaining seven patches labeled a, c, d, h, i, j and k are masked patches **314**. The present application is also applicable to other numbers of patches after the splitting and to other numbers of unmasked and masked patches.

[0088] The encoder ϵ .sub. θ **330** includes a set of learnable parameters θ . The encoder **330** is applied to the second image I.sub.2 **320** by applying the encoder **330** to the set of patches p.sub.2, thereby encoding the set of patches p.sub.2 into a representation ϵ .sub. θ (p.sub.2) **350** of the image I.sub.2 **320**. The set of patches P.sub.2 are encoded in a set of patch representations **252** forming the representation ϵ .sub. θ (p.sub.2) **350** of the image I.sub.2 **320**. The encoder **330** may encode each patch **322** of the set of patches P.sub.2 individually into a corresponding patch representation **252** such that the encoder **330** creates one patch representation **252** (e.g., a feature vector) per patch **322** of the set of patches p.sub.2.

[0089] The same encoder ϵ .sub. θ **330** is also applied to image I.sub.1 **310** to independently encode the first image I.sub.1 **310** in a representation **340** of image I.sub.1 **310**. However, in this case, the encoder **330** is only receives the set of remaining unmasked patches {tilde over (p)}.sub.1, thereby encoding the set of unmasked patches {tilde over (p)}.sub.1 into the representation ϵ .sub. θ ({tilde over (p)}.sub.1) **340** of the image I.sub.2 **310**. The set of patches {tilde over (p)}.sub.1 are encoded in a set of patch representations **342** forming the representation ϵ .sub. θ ({tilde over (p)}.sub.1) **340** of the image I.sub.1 **310**. The encoder **330** may encode each patch of the set of patches {tilde over (p)}.sub.1 individually into a corresponding patch representation **342** such that the encoder **330** creates one patch representation **242** (e.g., a feature vector) per patch of the set of unmasked patches {tilde over (p)}.sub.1.

[0090] In an example, the encoder **330** may be implemented with the Vision Transformer (ViT) architecture, such as described in Dosovitskiy et al., An Image is Worth 16×16 Words: Transformers for Image Recognition at Scale, ICLR, **2021**, which is incorporated herein in its entirety. The image patches may be used as tokens for the ViT backbone. In accordance with the ViT approach, the encoder **330** may include a linear projection on the input tokens (the patches **322** of the set p.sub.2 or the unmasked patches **312** of the set {tilde over (p)}.sub.1) to which sinusoidal positional embeddings may be added, followed by a series of transformer blocks (e.g.

self-attention followed by a Multi-Layer Perceptron (MLP)). Sinusoidal positional embeddings are described in Vaswani et al., Attention is all you need, NeurIPS, 2017, which is incorporated herein in its entirety.

[0091] The cross-view completion block **360** receives representation $\varepsilon.\text{sub}.\theta(\{\text{tilde over } (p)\}.\text{sub}.1)$ **340** and optionally representation $\varepsilon.\text{sub}.\theta(p.\text{sub}.2)$ **350**. The CroCo completion block **360** leaves representation $\varepsilon.\text{sub}.\theta(p.\text{sub}.2)$ **350** unaltered and forwards the representation to the decoder **370**. Additionally, the CroCo block **360** transforms representation $\varepsilon.\text{sub}.\theta(\{\text{tilde over } (p)\}.\text{sub}.1)$ **340** into transformed representation $\varepsilon.\text{sub}.\theta(\{\text{tilde over } (p)\}.\text{sub}.1)'$ **364**, such as by padding representation $\varepsilon.\text{sub}.\theta(\{\text{tilde over } (p)\}.\text{sub}.1)$ **340** with learned patch representations **362** (e.g., learned feature vectors) corresponding to the masked patches of image $I.\text{sub}.1$ **310**. In an example, representation $\varepsilon.\text{sub}.\theta(\{\text{tilde over } (p)\}.\text{sub}.1)$ **340** is padded with one learned representation **362** (e.g., a learned feature vector) for each masked patch of image $I.\text{sub}.1$ **310**. As the dimension of the patch representations used as input by the decoder **370** may differ from the dimension of the patch representations generated by the encoder **330**, the CroCo block **360** may perform a further transformation on $\varepsilon.\text{sub}.\theta(p.\text{sub}.2)$ and $\varepsilon.\text{sub}.\theta(\{\text{tilde over } (p)\}.\text{sub}.1)'$, such as by applying a fully-connected layer to the patch representations to project them to a predetermined input dimension for the decoder **370**.

[0092] Cross-view completion block **360** provides the transformed representation $\varepsilon.\text{sub}.\theta(\{\text{tilde over } (p)\}.\text{sub}.1)'$ **364** to the decoder **370**. Additionally, the decoder **370** receives representation $\varepsilon.\text{sub}.\theta(p.\text{sub}.2)$ **350** either directly from the encoder **330** or via the cross-view completion block **360**. In the following, the decoder **370** is denoted $D.\text{sub}.\phi$, which indicates that decoder $D.\text{sub}.\phi$ **370** includes a set of learnable parameters ϕ . The decoder **370** decodes transformed representation $\varepsilon.\text{sub}.\theta(\{\text{tilde over } (p)\}.\text{sub}.1)'$ **364** conditioned on $\varepsilon.\text{sub}.\theta(p.\text{sub}.2)$ **350** into a reconstruction $\{\text{circumflex over } (p)\}.\text{sub}.1$ of the set of patches $p.\text{sub}.1$, thereby generating a reconstructed image **380** as a patch-wise reconstruction of image $I.\text{sub}.1$ **310**, which may be expressed as:

$$\{\text{circumflex over } (p)\}.\text{sub}.1 = D.\text{sub}.\phi(\varepsilon.\text{sub}.\theta(\{\text{tilde over } (p)\}.\text{sub}.1)'; \varepsilon.\text{sub}.\theta(p.\text{sub}.2)) \quad (1)$$

[0093] In an example, the transformed representation $\varepsilon.\text{sub}.\theta(\{\text{tilde over } (p)\}.\text{sub}.1)'$ **364** is fed to a series of decoder transformer blocks (transformer modules (modules having the transformer architecture) of the decoder). Each block may include: (a) self-attention on the patch representations of $\varepsilon.\text{sub}.\theta(\{\text{tilde over } (p)\}.\text{sub}.1)'$ **364** including the patch representations **342** of image representation $\varepsilon.\text{sub}.\theta(\{\text{tilde over } (p)\}.\text{sub}.1)$ **340** and the added learned patch representations **362** corresponding to the masked patches **314** of $p.\text{sub}.1$; (b) cross-attention with the patch representations of $\varepsilon.\text{sub}.\theta(p.\text{sub}.2)$ **340**; and (c) a Multi-Layer Perceptron (MLP).

[0094] The set of learnable encoder parameters θ , the set of learnable decoder parameters ϕ , and the parameters of the learned patch representations of transformed representation $\varepsilon.\text{sub}.\theta(\{\text{tilde over } (p)\}.\text{sub}.1)'$ are updated by the training module **50** via back-propagation **144** based on the pretext loss **142**, as described with reference to FIG. 2.

[0095] In an example, the respective pretext loss may be determined by the training module **50** based on a patch-wise comparison of $\{\text{circumflex over } (p)\}.\text{sub}.1$ and $p.\text{sub}.1$ for the unmasked patches based on a metric that quantifies the difference of a patch $\{\text{circumflex over } (p)\}.\text{sub}.1.\text{sup}.i$ of $\{\text{circumflex over } (p)\}.\text{sub}.1$ and the corresponding masked patch $p.\text{sub}.1.\text{sup}.i$ of $p.\text{sub}.1$. In an example, the pretext loss for images $I.\text{sub}.1$ and $I.\text{sub}.2$ is evaluated as a Mean Square Error (MSE) loss between the pixels of a reconstructed patch $\{\text{circumflex over } (p)\}.\text{sub}.1.\text{sup}.i$ of $\{\text{circumflex over } (p)\}.\text{sub}.1$ and the corresponding pixels of the corresponding masked patch $p.\text{sub}.1.\text{sup}.i$ of $p.\text{sub}.1$ averaged over all unmasked patches of $p.\text{sub}.1$, such as described by the equation

$$[00001] \mathcal{L}(I_1, I_2) = \frac{1}{\text{Math. } p_1 \cdot \text{Math. } p_1} \cdot \text{Math. } \sum_{p_1^i \in p_1} (p_1^i - p_1^i)^2 \quad (2)$$

[0096] Alternatively, the pretext loss may be determined by the training module **50** by normalizing

the reconstructed patches $\{\text{circumflex over (p)}\}.\text{sub.1}$ and the corresponding masked patches $p.\text{sub.1}.\text{sup.i}$ of $p.\text{sub.1}$ within each patch, such as according to the mean and standard deviation of all pixels in a given patch. Based on the normalization values for each patch, the Mean Square Error (MSE) loss between the reconstructed patches $\{\text{circumflex over (p)}\}.\text{sub.1}.\text{sup.i}$ of $\{\text{circumflex over (p)}\}.\text{sub.1}$ and their respective corresponding unmasked patches $p.\text{sub.1}.\text{sup.i}$ of $p.\text{sub.1}$ are determined and averaged by the training module **50** over all unmasked patches of $p.\text{sub.1}$.

[0097] The pre-trained CroCo machine learning model can subsequently be used for supervised fine-tuning a task specific machine learning model for a downstream geometric vision task as detailed in the fine-tuning process **150** of FIG. **1**. Distinguishable may be fine-tuning for monocular tasks, which create predictions for a single image (e.g., monocular depth estimation, where a depth-map is predicted for a single image) and fine-tuning for tasks that need more than one image as input (e.g., two images). In the monocular fine-tuning scenario, the input image may be split into non-overlapping patches (e.g. 4×4 , 8×8 , 16×16 or 32×32 pixel patches) by the splitting module **300** and input to a ViT encoder, which is initialized by the training module **50** from the parameters of the pre-trained encoder **330** learned with self-supervision. Subsequently, the ViT encoder is fine-tuned by the training module **50** on the downstream task. For dense prediction tasks, the task specific machine learning model may be provided with a final fully-connected layer as prediction head that processes each patch representation produced by the ViT encoder independently and outputs the required predictions per pixel in each patch representation. This final output layer is trained by the training module **50** from scratch, unlike the ViT encoder.

[0098] CroCo pre-training can also be used for downstream tasks that involve a pair of images as input (e.g., optical flow). In this case, each input image is split by the splitting module **300** into non-overlapping patches (e.g. 4×4 , 8×8 , 16×16 or 32×32 pixel patches). The task specific machine learning model includes a task specific encoder with the same structure as the encoder **330**. The task specific encoder is initialized by the training module **50** with the parameter values of the pre-trained encoder **330**. The encoder **330** of the task specific machine learning model encodes the patches of each image of the image pair in a respective representation, each including a set of patch representations.

[0099] The task specific machine learning model further includes a task specific decoder, which has the same structure as the decoder **370**. The task specific decoder is initialized by the training module **50** with the parameter values of the pre-trained decoder **370**. The patch representations of the representation of the first image are processed by the decoder **370** using cross-attention computed with respect to the patch representations of the representation of the second image.

[0100] A final layer may be included as prediction head to project the outputs of the decoder **370** to a predetermined dimension and shape.

[0101] For the training, the CroCo machine learning model may be pre-trained for 200 or another suitable number of epochs, such as using the AdamW optimizer. A cosine learning rate schedule with a base learning rate of $1.5\times 10.\text{sup.}-4$ may be used for an effective batch size of 256.

Additionally, a linear warmup in the first 40 epochs may be performed. A ViT-Base backbone may be used as encoder including a series of 12 transformer blocks (modules) with 768 dimensions and 12 heads for self-attention, with patches of size 16×16 pixels. For the decoder, a series of 8 decoder blocks (modules) with 512 dimensions and 16 heads for both self- and cross-attention may be used.

[0102] The CroCo machine learning model may be pre-trained on a dataset including image pairs of indoor scenes. The pre-trained encoder may be kept as the initial encoder of a task specific machine learning model as part of which the pre-trained encoder is then fine-tuned to perform monocular depth estimation. For the downstream task optical flow estimation, both the pre-trained encoder and the pre-trained decoder may be kept as the initial encoder and decoder of a task specific machine learning model for optical flow estimation. Both the encoder and the decoder are later fine-tuned by the training module **50** to perform optical flow estimation given pairs of images.

[0103] The performance of the pre-trained CroCo model may be evaluated when fine-tuned for the task of monocular depth estimation. In this example, the task specific machine learning model generates 256 values (depth predictions) per patch. The final outputs are exponentiated by the model to enforce that depth predictions are positive. Subsequently, the training module 50 selectively trains the model based on minimizing an MSE (mean squared error) loss between predictions and ground-truth depth values. Additionally, the pre-trained CroCo model may be evaluated by fine-tuning it for optical flow estimation, by predicting two values per pixel in each patch using the prediction head. An MSE loss may be minimized by the training module 50 for fine-tuning. The experimental results show that the CroCo pretext task allows to pre-train task specific models for downstream geometric vision tasks more effectively than other methods by taking advantage of lower-level geometric cues.

TABLE-US-00001 TABLE 1 Ablation of the masking ratio (i.e., the ratio of the number of masked patches for image I.sub.1 to the total number of patches for image I.sub.1). Masking Depth Flow ratio r Acc @1.25 (%)↑ MSE (.Math.10.sup.-4)↓

Masking ratio r	Acc @1.25 (%)↑	MSE (.Math.10.sup.-4)↓
75%	80.29	7.3390
80%	81.44	7.1615
85%	82.03	7.0951
90%	83.51	6.8745
95%	83.14	6.6488

[0104] The experiments may be performed on synthetic images of 3D indoor scenes. In each 3D scene, up to 1000 pairs of camera viewpoints with a co-visibility greater than 50% may be randomly sampled. These pairs of viewpoints may be rendered using a Habitat simulator. In an example, a total of 1,821,391 pairs for pre-training may be generated from different indoor scenes.

[0105] Additionally, in an example a training (and respectively test) set for downstream tasks of 200,000 (resp. 20,000 pairs) may be created for other indoor scenes. For monocular depth estimation, the downstream task specific model may be fine-tuned on 20,000 images, while 2,000 images may be used for fine-tuning for optical flow estimation. Images of size 256×256 pixels may be generated and crops of size 224×224 may be used. For monocular depth estimation, Acc@1.25 is reported, which may involve the ratio of pixels fulfilling the condition $\max(d/d, d/d) < 1.25$, with d and d the predicted and ground-truth depth respectively. For optical flow estimation, the Mean Square Error (MSE) loss is reported.

[0106] In Table 1 above, the impact of the masking ratio r is illustrated. Note that 75% masking may provide accuracy in the context of auto-completion for MAE. Overall, high masking ratios of 90% or 95% better performance of the CroCo model.

[0107] In Table 2 below, additionally the performance of the CroCo approach is evaluated when normalizing the targets and when varying the decoder depth, i.e., the number of decoder blocks in D.sub.φ. Normalizing the targets may improve performance for both downstream tasks. While the decoder depth may have only minimal impact for the monocular task, a sufficiently deep decoder may be used for tasks that take pairs of images as input, such as optical flow, as it also increases the model capacity.

TABLE-US-00002 TABLE 2 Impact of normalizing targets and decoder depth with 90% masking ratio. norm. decoder Depth Flow target depth Acc @1.25 (%)↑ MSE (.Math.10.sup.-4)↓

norm.	decoder	Depth	Flow	target	depth	Acc @1.25 (%)↑	MSE (.Math.10.sup.-4)↓
X	8	83.51	6.8745	✓	8	84.67	6.2924
✓	6	83.70	7.1711	✓	4	83.33	10.337
✓	2	85.8	13.219				

[0108] The CroCo pre-training method evaluated on downstream tasks is compared to training from scratch as well as another model (MAE) in Table 3 below. The other model may be pre-trained and additionally fine-tuned with supervision for image classification on this dataset, or pre-trained on a dataset such as the same images that are used for pre-training according to the CroCo approach. A benefit of pre-training for both tasks has been observed compared to training from scratch with, for instance, a difference of about 20% for depth accuracy at the 1.25 threshold. CroCo pre-training may provide superior performance than the other model for geometric tasks, with a gain of about 1% for depth accuracy at 1.25. Also, results are obtained that are two orders of magnitude better for optical flow estimation.

TABLE-US-00003 TABLE 3 Comparison to other (MAE) with ViT-B encoder. Depth Flow Acc @1.25 (%)↑ MSE (.Math.10.sup.-4)↓

Method	Depth Acc @1.25 (%)↑	Flow MSE (.Math.10.sup.-4)↓
from scratch	62.66	275
MAE pretrained	77.19	152

[0109] The cross-view alignment (Caiman) pre-training system as illustrated in FIG. 4 is another example implementation of unsupervised pre-training 110. The pretext machine learning model for Caiman pre-training may be referred to as the Caiman machine learning model. The Caiman machine learning model corresponds to pretext machine learning model 130, as illustrated in FIG. 2. The Caiman machine learning model includes an encoder (module) 430 (corresponding to encoder 230), a decoder (module) 470 (corresponding to decoder 270) and a cross-view alignment block (module) 460 (corresponding to representation space block 260). The encoder 430 includes a set of learnable encoder parameters θ , and the decoder 470 includes a set of learnable decoder parameters ϕ .

[0110] The Caiman machine learning model is applied to a pair of unannotated images including a source image $I_{\text{sub.S}}$ 410 and a target image $I_{\text{sub.T}}$ 420. The two images depict the same visual content (e.g., a same scene, a same object, a same person, or a same architectural structure) from different viewpoints or from a similar viewpoint at different times or under different conditions (e.g., lighting conditions, seasonal conditions, depth of field, focal length, etc.). The pixel dimensions of the two images may be equal or may differ from each other. The images 410 and 420 do not need to include additional annotations with ground-truth data according to the Caiman task since the Caiman pre-training is performed unsupervised.

[0111] The source image $I_{\text{sub.S}}$ 410 is encoded into source representation $x_{\text{sub.S}}$ 440 by the encoder 430. The encoder 430 independently encodes target image $I_{\text{sub.T}}$ 420 into target representation $x_{\text{sub.T}}$ 450. In an embodiment, source representation $x_{\text{sub.S}}$ 440 may be an ordered set of n K -dimensional vectors 442, $x_{\text{sub.S}} = \{x_{\text{sub.S},i}\}_{i=1, \dots, n}$, where $x_{\text{sub.S},i} \in \mathbb{R}^K$. Similarly, target representation $x_{\text{sub.T}}$ 450 may be an ordered set of n K -dimensional vectors 452, $x_{\text{sub.T}} = \{x_{\text{sub.T},i}\}_{i=1, \dots, n}$, where $x_{\text{sub.T},i} \in \mathbb{R}^K$. The number of vectors n and their dimension K are adjustable parameters of the Caiman pre-training method and can be set to any suitable value. In an example embodiment, $n=512$ and $K=128$.

[0112] In an example implementation of the encoder 430, the source and target representations may be generated using an architecture based on Perceiver IO, described in Jaegle et al., "Perceiver 10: A General Architecture for Structured Inputs & Outputs", ICLR, 2022, which is incorporated herein in its entirety. For example, a two dimensional (2D) convolution layer (e.g., a 5×5 , 6×6 , 7×7 , or 9×9 2D convolution layer) and a Rectifier Linear Unit (ReLU) activation may be applied to an input image (e.g. source image $I_{\text{sub.S}}$ 410 or target image $I_{\text{sub.T}}$ 420) to produce a feature map, where the feature map may include one feature vector for each pixel of the input image. The dimension of the feature vector may be a predetermined parameter of the encoder and may be a suitable number. In some examples, the dimension of the feature vector is 32, 64, 128, or 256. The feature map may be split into patches of feature vectors (e.g., into non-overlapping quadratic patches of sizes 8×8 , 12×12 , 16×16 , 20×20 or 32×32) by the splitting module 300. Each patch may be associated with a Fourier positional encoding. The patches are subsequently used to modify a set of n randomly initialized vectors of dimension K through cross-attention to produce a representation x of the input image (e.g. source image $I_{\text{sub.S}}$ 410 or target image $I_{\text{sub.T}}$ 420), updated by applying a block of self-attention layers (e.g. 4, 6, 8, 10 or 12 self-attention layers).

[0113] The source representation $x_{\text{sub.S}}$ 440 and the target representation $x_{\text{sub.T}}$ 450 are provided to the cross-view alignment block 460. Cross-view alignment block 460 transforms source representation $x_{\text{sub.S}}$ 440 into transformed source representation $\hat{x}_{\text{sub.S}}$ 468 by applying transformation h 466 to source representation $x_{\text{sub.S}}$ 440. Transformation h 466 includes a set of transformation parameters Ω 464, which are configured to transform source representation $x_{\text{sub.S}}$ 440 such that the resulting transformed source representation $\hat{x}_{\text{sub.S}}$ 468 approximates (e.g., aligns with) target representation $x_{\text{sub.T}}$ 450. In order to achieve alignment between transformed source

representation $\{\text{circumflex over (x)}\}.\text{sub.S}$ **468** and target representation $x.\text{sub.T}$ **450**, parameter module g **462** determines the parameters Ω **464** of the transformation h based on the source representation $x.\text{sub.Ss}$ **440** and the target representation $x.\text{sub.T}$ **450**, or in mathematical terms, $\Omega = g(x.\text{sub.S}, x.\text{sub.T})$. The determined parameters Ω **464** are input to the transformation h **466** to transforms source representation **442** into transformed source representation **468**.

[0114] In an example of the cross-view alignment block **460**, it is assumed that each vector $x.\text{sub.i} \in \text{custom-character}.\text{sup.K}$ can be decomposed into two parts, an equivariant part $x.\text{sub.i}.\text{sup.equiv} \in \text{custom-character}.\text{sup.D}$ and an invariant part $x.\text{sub.i}.\text{sup.inv} \in \text{custom-character}.\text{sup.K-D}$, where $0 < D \leq K$. The invariant part may be constant across different views of the same scene, contrary to the equivariant part, which may change across the source and target views. One possible example for transformation $h.\text{sub}.\Omega$ **466** is a D -dimensional rotation. However, the present application is also applicable to other transformations, and a more complex transformation may be chosen instead (e.g., more general D -dimensional affine or geometric transformations). With the above, transformation $h.\text{sub}.\Omega$ **466** is given as a D -dimensional rotation matrix Ω and applying transformation $h.\text{sub}.\Omega$ **466** to source representation $x.\text{sub.S}$ **440** amounts to multiplying the equivariant part of each representation vector $x.\text{sub.S},i.\text{sup.equiv}$ with rotation matrix Ω . Given the representations $x.\text{sub.S}$ and $x.\text{sub.T}$ of the source and target images $I.\text{sub.S}$ and $I.\text{sub.T}$, the rotation matrix Ω that best aligns the equivariant parts of the source and target representations may be estimated as:

$$[00002] \quad \Omega = \arg \min_{\hat{\Omega} \in SO(D)} \sum_{i=1}^n \|\hat{\Omega} x_{S,i}^{\text{equiv}} - x_{T,i}^{\text{equiv}}\|^2 \quad (3)$$

$SO(D)$ denotes the D -dimensional special orthogonal group, which includes all possible D -dimensional rotation matrices. The rotation may be estimated using a closed and differentiable form, such as described in Schönemann, A generalized solution of the orthogonal Procrustes problem, Psychometrika, 1966, or Umeyama, Least-squares estimation of transformation parameters between two point patterns, TPAMI, 1991, or Brégier, Deep regression on manifolds: a 3D rotation case study, 3DV, 2021, which are incorporated herein in their entirety. This allows to align source representation $x.\text{sub.S}$ **440** to target representation $x.\text{sub.T}$ **450**. Specifically, the transformed source representation $\{\text{circumflex over (x)}\}.\text{sub.S}$ **468** can be determined by the cross-view alignment block **460** as follows: $\{\text{tilde over (x)}\}.\text{sub.S} \cong (\Omega x.\text{sub.S}.\text{sup.equiv}, x.\text{sub.S}.\text{sup.inv})$.

[0115] To solve the cross-view alignment task, the Caiman machine learning model extracts some transformation parameters representing how the source and target images are related (the rotation matrix Ω). This enables the model to encode changes of viewpoints, lighting, etc. between views. In some embodiments, the transformation h is constrained to have a predetermined number of degrees of freedom. This predetermined number is an adaptable parameter of the Caiman pre-training procedure and can be set to any suitable number. In the above exemplary implementation, this constrained number of degrees of freedom amounts to constraining D to a predetermined number (e.g. 24).


[0116] Once the source representation $x.\text{sub.S}$ **440** has been transformed into transformed source representation $\{\text{circumflex over (x)}\}.\text{sub.S}$ **468**, decoder **470** decodes transformed source representation $\{\text{circumflex over (x)}\}.\text{sub.S}$ **468** into reconstructed image $I.\text{sub.R}$ **480**. In an example implementation of the decoder, transformed source representation $\{\text{circumflex over (x)}\}.\text{sub.S}$ **468** is decoded into a feature map using a patch-based approach. The feature map may include one feature vector of a predetermined dimension (e.g. 32, 64, 128, or 256) for each pixel of the reconstructed image. For each patch of a predetermined patch size (e.g. 8×8 , 12×12 , 16×16 , 32×32 pixels) of the feature map, a flattened representation of the features map values for this patch are generated (e.g., by a flattening module), such as by performing a cross-attention between $\{\text{circumflex over (x)}\}.\text{sub.S}$ and a Fourier encoding of the patch 2D position. The flattened

representations are merged (e.g., by a merging module) into a single feature map, and a 2D convolution layer with a predetermined convolution kernel size (e.g. 5×5, 7×7, 9×9) is applied to produce the final reconstructed RGB image. The reconstructed image may have the same pixel dimensions as the target image I.sub.T **420**.

[0117] The set of learnable encoder parameters θ and the set of learnable decoder parameters p are updated by the training module **50** by back-propagation (e.g., back-propagation **144**) based on a pretext loss (e.g. pretext loss **142**). The loss for Caiman pre-training (the Caiman loss) may be determined by the training module **50** based on a comparison of the reconstructed image I.sub.R **480** to the target image I.sub.T **420**, e.g. based on a metric (e.g., the Mean Square Error metric) quantifying the deviation of the reconstructed image I.sub.R **480** from the target image I.sub.T **420**. Additionally, or alternatively, the Caiman loss may be determined by the training module **50** based on a comparison of the transformed source representation x.sub.S **468** to the target representation x.sub.T **450**, e.g. based on a metric (e.g. the Mean Square Error metric) quantifying the deviation of the, transformed source representation $\{\tilde{x}\}$.sub.S **468** from the target representation x.sub.T **450**. In one embodiment, the Caiman loss may be determined by the training module **50** using the equation:

[00003]

$$\mathcal{L}(I_S, I_T) = \sum_{i=1}^{H \times W} \mathcal{L}_{\delta}(I_R(i) - I_T(i)) + \lambda \|x_S - x_T\|_2, \quad (4)$$

where I.sub.R(i) correspond to the red green blue (RGB) values of the reconstructed image I.sub.R**480** at the pixel position i and equivalently, I.sub.T(i) correspond to the RGB values of the target image I.sub.T **420** at the pixel position i.  custom-character.sub.δ is the Huber loss:

$$[00004] \mathcal{L}_{\delta}(a) = \begin{cases} \frac{1}{2}a^2 & \text{for } |a| \leq \delta \\ \delta \cdot (|a| - \frac{\delta}{2}) & \text{otherwise} \end{cases} \quad (5)$$

In an example $\delta=0.1$. However, another suitable value for $\delta=0.1$ may be used.

[0118] The pre-trained Caiman machine learning model (specifically pre-trained encoder **430** and pre-trained decoder **470**) can be used for supervised fine-tuning of a task specific machine learning model for a downstream geometric vision task, as detailed in the fine-tuning process **150** of FIG. **1**. One may distinguish between fine-tuning for monocular tasks, which create predictions for a single image (e.g., monocular depth estimation, where a depth-map is predicted for a single image) and fine-tuning for tasks that use multiple images as input (e.g., two images). In the monocular fine-tuning scenario, the task specific machine learning model may include an encoder and a decoder, both having the same structure as their counterparts in the Caiman machine learning model. The encoder parameters of the encoder of the task specific machine learning model are initialized with the parameters of the pre-trained encoder of the Caiman machine learning model. Similarly, the decoder parameters of the decoder of the task specific machine learning model are initialized with the parameters of the pre-trained decoder of the Caiman machine learning model. The task specific model for monocular downstream geometric vision tasks (e.g. monocular depth estimation) may include a final convolutional layer outputting a single channel (e.g., the depth). This final layer may be trained by the training module **50** from scratch, while the encoder and the decoder are initialized by the training module **50** with the pre-trained (predetermined) parameters. The encoder is applied to the input image to generate a representation of the input image. The decoder, together with the final layer, generates the output data (e.g., the depth data).

[0119] CroCo pre-training can also be used for downstream tasks that require a pair of images as input (e.g., relative pose estimation). In the example of relative camera pose estimation, the downstream geometric vision task includes estimating the relative camera displacement between two views of the same scene. Cross-view alignment provides a pre-training task that is close to the problem of relative pose estimation, and a model pre-trained with Caiman can be fine-tuned to

determine a relative rotation $R \in \text{SO}(3)$ and a relative translation $t \in \mathbb{R}^3$ between two views of a given scene for a given camera.

[0120] In the task specific machine learning model for pose estimation, the two images are independently fed into the task specific encoder, which may have the same structure as the encoder 430 of the Caiman machine learning model, and is initialized by the training module 50 with the parameters of the pre-trained Caiman encoder 430. The two representations generated are input into the parameter module g 462 to estimate the alignment parameter Ω between the two image representations. This parameter is given as input of a rotation and a translation head that determines, for example, a 3×3 matrix and a 3D translation vector t , respectively. These heads may be implemented using Multi-Layer Perceptrons (MLPs) in various implementations with a predetermined number of hidden layers (e.g., 64, 128, 196, 256). The 3×3 matrix is further orthonormalized into a rotation matrix R using the special orthogonal Procrustes orthonormalization, such as described in Brégier, Deep regression on manifolds: a 3D rotation case study”, 3DV, 2021, which is incorporated herein in its entirety.

[0121] The downstream model is fine-tuned by the training module 50 in a supervised manner to minimize a pose estimation error such as:

$$[00005] \mathcal{L}_P = \text{Math. } R - R_{\text{gt}} \text{Math. }^2_F + \lambda \text{Math. } t - t_{\text{gt}} \text{Math. }^2_F \quad (6)$$

with respect to the ground truth relative pose $(R_{\text{sub.gt}}, t_{\text{sub.gt}}) \in \text{SO}(3) \times \mathbb{R}^3$. In one embodiment $\lambda = 0.1$. However, another suitable value may be used.

[0122] The following presents experimental results for monocular depth estimation and pose estimation pre-trained with the described self-supervised Caiman process. The experimental results have been achieved with an implementation of the Caiman model in PyTorch. The Caiman machine learning model may be pre-trained with the RAdam optimizer.

TABLE-US-00004 TABLE 4 Error of relative pose estimation for different training set sizes.

Training	10 k	20 k	30 k	60 k	From scratch
	19.1°	0.99 m	17.4°	0.91 m	15.3°
	0.81 m	14.0°	0.73 m		
Fine-Tuning	19.0°	0.93 m	16.2°	0.81 m	12.7°
	0.67 m	11.5°	0.61 m		

[0123] The experiments may be performed on synthetic images of 3D indoor scenes. In each scene, up to 1,000 pairs of camera viewpoints with a co-visibility greater than 50% have been randomly sampled. These pairs of viewpoints have been rendered using a simulator. Images of size 256×256 may be used and random crops of size 224×224 may be used as input images. In total, 800,000 pairs from different indoor scenes may be used for pre-training the Caiman machine learning model. While example numbers of pairs, viewpoints, samplings, and sizings have been provided, the present application is also applicable to other values.

[0124] For the relative pose estimation downstream task, a training (resp. test) set may include 200,000 (resp. 20,000) pairs may additionally be created, in a similar manner, from indoor scenes unseen during the Caiman pre-training process. To evaluate the performances for relative pose estimation of a model, subsets of different sizes may be considered and the task specific machine learning model may be fine-tuned for 100 epochs.

[0125] Table 4 compares the results obtained when training the task specific machine learning model for relative pose estimation from scratch (including the encoder and the decoder) with results obtained when the task specific model was fine-tuned from a pretext machine learning model pre-trained using the described cross-view alignment process. Table 4 illustrates that the pre-training is consistently beneficial to the performance of the model for this task.

[0126] For monocular depth estimation, the respective task specific machine learning model may be fine-tuned on 20,000 images randomly selected from the downstream task training set used for relative pose estimation. The fine-tuned task specific machine learning model may be evaluated on the corresponding test set. To evaluate the quality of the predicted depth, the $\text{Acc}@1.25$ may be used, involving the ratio of pixels satisfying $\max(d/d, d/d) < 1.25$, with d and d the predicted and ground-truth depth, respectively.

[0127] The performance of the Caiman pre-training may be empirically evaluated for the downstream geometric vision task of monocular depth estimation. The task specific machine learning model outputs scalar values that are exponentiated (e.g., input to an exponential function) to enforce positive depth predictions. The task specific model may be fine-tuned by the training module **50** to minimize a MSE loss between depth predictions and ground-truth depth values, such as in log-space. In Table 5, the performance obtained when training the task specific machine learning model for monocular depth estimation from scratch (both encoder and decoder) is compared to the performance of a task specific machine learning model when Caiman pre-trained. A performance gain when using the pre-trained model is observed, with performance increasing from 0.39 to 0.48.

TABLE-US-00005 Depth Training Acc @1.25 (%) From scratch 0.39 Fine-Tuning 0.48

[0128] FIG. **5** is a flowchart illustrating a computer-implemented method **500** of training a task specific machine learning model for a downstream geometric vision task. The method begins with **510** with the training module **50** performing unsupervised pre-training of a pretext machine learning model (e.g., pretext machine learning model **130**). In an example, the unsupervised pre-training may be self-supervised pre-training. The pretext machine learning model includes an encoder (e.g., encoder **230**, **330**, or **430**) and a decoder (e.g., decoder **270**, **370**, or **470**). The encoder has a set of encoder parameters and the decoder has a set of decoder parameters. The unsupervised pre-training may be performed according to unsupervised pre-training **110** of FIG. **1**. [0129] At **520**, a task specific machine learning model (e.g., task specific machine learning model **170**) is constructed or obtained for a downstream geometric vision task (e.g., a 3D geometric task in computer vision such as depth estimation, optical flow estimation, or relative pose estimation) based on the pre-trained pretext machine learning model. The task specific machine learning model includes a task specific encoder having a set of task specific encoder parameters. The task specific machine learning model may additionally include a task specific decoder having a set of task specific decoder parameters. In some embodiments the task specific encoder has the same structure as the encoder of the pretext machine learning model. Additionally, the task specific decoder may have the same structure as the decoder of the pretext machine learning model.

[0130] The method continues at **530** with the training module **50** initializing the set of task specific encoder parameters with the set of encoder parameters of the pre-trained pretext machine learning model. In some embodiments the set of task specific decoder parameters are initialized by the training module **50** with the set of decoder parameters of the pre-trained pretext machine learning model.

[0131] At **540**, the task specific machine learning model is fine-tune trained by the training module **50** for the downstream geometric vision task. In some embodiments, the fine-tuning is performed as supervised fine-tuning, which is based on a training data set of annotated images or pairs of annotated images in accordance with supervised fine-tuning **150** of FIG. **1**.

[0132] Performing the fine-tuning of the task specific machine learning model for the downstream geometric vision task starts with applying the task specific machine learning model to one or more images (e.g., annotated images). For monocular downstream geometric vision tasks (e.g., monocular depth estimation) the task specific machine learning model may be applied to one input image; for binocular downstream geometric vision tasks (e.g., binocular depth estimation, relative pose estimation, image flow estimation) the task specific machine learning model may be applied to a pair of input images. The images of the image pair may depict a same visual content (a same scene) but may have been taken from different viewpoints or from a similar viewpoint at different times or under different conditions (e.g., different focal length, different depth of field, different lighting conditions, different seasons).

[0133] The task specific encoder may generate a respective image representation for each input image. In some examples, the one or more image representations are input into the task specific decoder to generate a decoded image representation. Either the one or more image representations

or the decoded image representation may be input to a task specific output layer of the task specific machine learning model (e.g., a 2D convolution layer or a Multi-Layer Perceptron) to create task specific output data (e.g., a depth map of the scene, a relative rotation matrix, and a relative translation vector) according to the downstream geometric vision task. The one or more annotated images are annotated with ground truth data corresponding to the downstream geometric vision task. The value of a task specific loss function may be determined by the training module **50** based on a metric quantifying (corresponding to) the difference between the created output data and the ground truth data. Subsequently, the task specific machine learning model is adjusted by the training module **50** adjusting the set of task specific encoder parameters (and optionally the set of task specific decoder parameters) of the task specific machine learning model, such as based on or to minimize the value of the task specific loss function.

[0134] The next iterative step may start with or include applying the adjusted task specific machine learning model to one or more annotated images to generate new task specific output data, determining a new value for the task specific loss function and further adjusting the learnable parameters of the task specific encoder (and optionally the task specific decoder). This iterative process stops either after a predetermined number of iterations (e.g., epochs), or when a minimum value of the task specific loss function is reached (the minimization of the loss function has converged).

[0135] Once the task specific machine learning model has been fine-tuned for the downstream geometric vision task, the model can be applied to perform the downstream geometric vision task on a set of images. The fine-tuned model is applied to one or more unannotated images in the same way as in an iteration step of the fine-tuning phase (e.g., fine-tuning **150**) to create task specific output (or prediction) data based on the input image(s). However, the determination of the value of the loss function and the iterative adjustment of the task specific machine learning model is not performed in the application phase.

[0136] In one example, the task specific machine learning model is fine-tuned for relative pose estimation. In this example, the fine-tuned task specific machine learning model is applied to a pair of new images that have not been part of the pre-training or fine-tuning data sets. The images of the pair of new images depict two views of the same scene (depict the same scene from different viewpoints and/or from a similar viewpoint at different times). By applying the fine-tuned model to the pair of new images, a relative rotation and a relative translation between the views of the images of the new pair of images is determined by the task specific machine learning model as the prediction data.

[0137] In an example, the downstream geometric vision task for which the task specific machine learning model is fine-tuned is depth estimation. Depth estimation can be performed in a monocular (using a single image) and a binocular (using two images) manner. In the monocular case, the fine-tuned task specific machine learning model is applied to a new image (which was not part of the pre-training or fine-tuning data sets) to extract a depth map of the new image as the prediction data. In the binocular case, the fine-tuned task specific machine learning model is applied to a pair of new images which depict the same scene from different viewpoints to extract a depth map for the depicted scene as the output prediction data.

[0138] In yet another example, the task specific machine learning model is fine-tuned for optical flow estimation. For this downstream geometric vision task, the fine-tuned task specific machine learning model is applied to a new image pair (which was not part of the pre-training or fine-tuning data sets) including a new first image and a new second image. The new first and second images depict the same scene under different conditions or from different viewpoints (or from a similar viewpoint at different times). When applied to the new image pair, the fine-tuned task specific machine learning model identifies a plurality of pixel pairs as the prediction data. Each pixel pair includes one pixel of the new first image and one corresponding pixel in new the second image, where the pixels of a pair correspond to the same visual feature of the depicted scene. From pairs of

pixels the motion of identified visual feature(s) of the depicted scene between the new first image and the new second image are determined by the task specific machine learning model.

[0139] In the following section, the pre-training **510** of FIG. 5 is discussed in more detail with reference to FIGS. 6, 7, and 8.

[0140] FIG. 6 is a flowchart illustrating a computer-implemented method **600** of pre-training a pretext machine learning model (e.g., pretext machine learning model **130**) for a pretext task. **600** provides an example implementation of unsupervised pre-training of **510** of FIG. 5. The pretext machine learning model includes an encoder (e.g., encoder **230**, **330**, or **430**) and a decoder (e.g., decoder **270**, **370**, or **470**). The encoder has a set of encoder parameters and the decoder has a set of decoder parameters.

[0141] The method begins with **610** with obtaining a pair of unannotated images including a first image (e.g., image **120**, **310**, or **410**) and a second image (e.g., image **122**, **320**, or **420**). The first and second images depict a same scene taken under different conditions (e.g., different focal length, different lighting conditions, different seasons) or from different viewpoints or from a similar viewpoint at different times.

[0142] At **620**, the encoder of the pretext machine learning model encodes the first image into a first representation (e.g., image representation **240**, **340**, or **440**). Additionally, the second image is encoded into a second representation (e.g., image representation **250**, **350**, or **450**) by the encoder.

[0143] The first representation is transformed into a transformed representation (e.g., transformed representation **264**, **364**, or **468**) at **630**. The transformation may be performed in representation space block **260**, cross-view completion block **360**, or cross-view alignment block **460**. The transformed representation is decoded into a reconstructed image (e.g., reconstructed image **140**, **380**, or **480**) by the decoder of the pretext machine learning model at **640**. The reconstructed image is based on the first and the second representation in that either the transformation of the first representation depends on the second representation or the decoder takes both the transformed representation and the second representation as input and decodes the first representation into the reconstructed image conditioned on the second representation.

[0144] At **650**, the encoder and the decoder are adjusted (i.e., updated or modified) by the training module **50** by adjusting their respective sets of encoder and decoder parameters based on or to minimize a loss function (minimize the value of the loss function (e.g., pretext loss **142**)). By adjusting the encoder and decoder parameters, the pretext machine learning model is adjusted such that it better performs the pretext task after the adjustment. The pretext machine learning model may include further learnable parameters, e.g., as part of a representation space block such as representation space block **260**. These optional additional learnable parameters are also adjusted based on minimizing the loss function. In order to minimize the loss function, the pretext loss (the value of the loss function) may be determined based on a deviation of the reconstructed image to an image it is meant to reconstruct (e.g., one of the images of the input image pair). Additionally or alternatively, the loss may be determined based on a deviation of the transformed representation to one of the image representations generated by applying the encoder to the images of the input image pair. Adjusting the learnable parameters of the pretext machine learning model (including the parameters of the encoder and the decoder) is performed by back propagation (e.g., back propagation **144**). After adjusting the pretext machine learning model, the process may stop or repeat. In case the process repeats, a new iteration is started **610** with the adjusted pretext machine learning model including the adjusted encoder and decoder. The process may stop after a predetermined number of iterations (e.g., epochs) or when a minimum value of the pretext loss function is reached (e.g., the value of the pretext loss function has converged towards or to a minimum value).

[0145] FIG. 7 is a flowchart depicting an example computer-implemented method **700** of performing cross-view completion pre-training of a pretext machine learning model (e.g., pretext machine learning model **130**) for the cross-view completion pretext task. Method **700** provides an

example implementation of pre-training **510** of FIG. **5** and is an example embodiment of method **600** for the specific pretext task of cross-view completion. The pretext machine learning model comprises an encoder (e.g. **330**) and a decoder (e.g. decoder **370**). The encoder has a set of encoder parameters and the decoder has a set of decoder parameters.

[0146] Method **700** starts at **710** with obtaining a pair of images including a first image (e.g., image **310**) and a second image (e.g., image **320**). The first and second images depict the same scene (the same visual content) and are taken under different conditions or from different viewpoints or from a similar viewpoint at different times. Accordingly, the two images of the pair of images show the same visual content but from different viewpoints or with different lighting, different depth of field, different focal length, or other differences. In particular, the pixel content of the two images of the image pair differs from each other but depicts the same scene. Each image of the image pair provides a distinct view of the depicted scene, which differs from the view provided by the other image of the pair.

[0147] At **720** the method continues with splitting the first image into a first set of non-overlapping patches (e.g., image patches **312**) and splitting the second image into a second set of non-overlapping patches (e.g., image patches **322**). At **730** a plurality of patches of the first set of patches is masked. In an example, a predetermined percentage (e.g., between 75% and 95%) of the patches of the first set of patches is randomly selected to be masked and masked.

[0148] After splitting the first image, the encoder encodes the first image at **740** into a first representation (e.g., image representation **340**) by encoding each remaining unmasked patch of the first set of patches into a corresponding representation (e.g., patch representation **342**) of the respective unmasked patch, thereby generating a first set of patch representations. Encoding the first image into the first representation comprises encoding only the unmasked patches into the first set of patch representations such that the first set of patches do not include patch representations for the masked patches (e.g., masked patches **314**).

[0149] At **750**, the encoder encodes the second image into a second representation (e.g., image representation **350**) by encoding each patch of the second set of patches into a corresponding representation (e.g., patch representation **352**) of the respective patch, thereby generating a second set of patch representations. **740** and **750** are an implementation of **620** of FIG. **6** for the CroCo pretext task.

[0150] At **760**, the first representation of the first image is transformed into a transformed representation (e.g., transformed representation **364**). In an example, the first representation is transformed into the transformed representation by padding the first set of patch representations, which includes only patch representations for unmasked patches of the first image, with a respective learned representation (e.g., learned representation **362**) for each of the masked patches of the first image. Each learned representation of a masked patch includes a set of learnable representation parameters. The resulting transformed representation may include each of the patch representations of the first set of patch representations (e.g., patch representation **342**) and additionally a plurality of learned patch representations corresponding to the masked patches (e.g., learned patch representation **362**).

[0151] Following the transformation of the first representation, the method continues at **770** with decoding, by the decoder, the transformed representation into a reconstructed image (e.g., reconstructed image **380**). The transformed representation is decoded by generating, for each masked patch of the first set of patches, a predicted reconstruction for the respective masked patch based on the first and second sets of patch representations. In an example, generating the predicted reconstruction of a masked patch of the first set of patches includes decoding, by the decoder, the learned representation of the masked patch into the predicted reconstruction of the masked patch. For decoding the learned representation of a masked patch, the decoder receives the first and second sets of patch representations as input data and decodes the learned representation of the masked patch based on the input data. In some examples, the transformed representation includes

the patch representations of the first set of patch representations and the transformed representation is decoded into the reconstructed image conditioned on the second representation.

[0152] At **780**, the encoder and the decoder are adjusted (e.g., updated or modified) by adjusting their corresponding sets of encoder and decoder parameters to minimize a loss function (e.g., minimize the value of the loss function (e.g., pretext loss **142**)). In an example, the loss function may be based on a metric quantifying the difference between each masked patch of the first image and its respective predicted reconstruction. In an example, the pretext machine learning model may include sets of learnable parameters of the learned representations corresponding to the masked patches of the first image. In this example, the additional learnable parameters and thereby the learned representations are also adjusted to minimize the loss function. By adjusting the encoder and decoder parameters and optionally the parameters of the learned representations, the pretext machine learning model is adjusted such that it better performs the cross-view completion task after the adjustment. Adjusting the learnable parameters of the pretext machine learning model (including the parameters of the encoder and the decoder) is performed by back propagation (e.g., back propagation **144**). After adjusting the pretext machine learning model, the process may stop or repeat. In case the process repeats, a new iteration is started at **710** for the adjusted pretext machine learning model including the adjusted encoder and decoder (and optionally the adjusted learnable representations). The process may stop after a predetermined number of iterations are completed or when a minimum value of the pretext loss function is reached (e.g., the value of the pretext loss function has converged towards or to a minimum value).

[0153] FIG. **8** includes a flowchart of an example computer-implemented method **800** of pre-training **510** of FIG. **5**, namely a computer-implemented method of performing cross-view alignment pre-training of a pretext machine learning model (e.g., pretext machine learning model **130**) for the cross-view alignment pretext task. Method **800** is an example of method **600** for the specific pretext task of cross-view alignment. The pretext machine learning model includes an encoder (e.g. encoder **430**) and a decoder (e.g. decoder **470**). The encoder has a set of encoder parameters and the decoder has a set of decoder parameters.

[0154] The method begins with **810** with obtaining a pair of images including a first image (e.g., source image **410**) and a second image (e.g., target image **420**), where the first and second images depict a same scene and are taken under different conditions or from different viewpoints or from a similar viewpoint at different times. Accordingly, the two images of the pair of images show the same visual content but from different viewpoints or with different lighting, different depth of field, different focal length, or other visual differences of the same scene. In particular, the pixel content of the two images of the image pair differs from each other but includes the same scene. Each image of the image pair provides a distinct view on the depicted scene, which differs from the view provided by the other image of the pair.

[0155] Method **800** continues at **820** with encoding, by the encoder of the pretext machine learning model, the first image into a first representation (e.g., source representation **440**) of the first image and the second image into a second representation (e.g., target representation **450**) of the second image. In an example, the first representation may be a first set (e.g., an ordered set) of n vectors $\{x_{sub.1,i}\}_{sub.i=1 \dots n}$, each $x_{sub.1,i} \in \mathbb{R}^{K}$. Equally, the second representation may be a second set (e.g., an ordered set) of n vectors $\{x_{sub.2,i}\}_{sub.i=1 \dots n}$, each $x_{sub.2,i} \in \mathbb{R}^{K}$.

[0156] At **830**, the first representation is transformed into a transformed representation (e.g., transformed source representation **468**) by applying a transformation (e.g., transformation **466**) to the first representation. The transformation is determined based on the first and second representations such that the transformed representation approximates (e.g., aligns with) the second representation. The transformation may depend on a set of transformation parameters (e.g., parameters Ω **464**) which may be determined by a parameter module (e.g., parameter module **462**) based on the first representation and the second representation. In some examples, each vector of

the first and second sets of vectors are decomposed in a D-dimensional equivariant part and a (K-D)-dimensional invariant part, where D is a natural number between one and K. In this example, applying the transformation includes decomposing each vector and applying a (D×D)-dimensional transformation matrix Ω to the equivariant part of each vector of the first set of vectors. Applying the transformation to any vector of the first and second sets of vectors does not change the invariant part of the respective vector. Applying the transformation matrix Ω to the equivariant part of a vector may be performed by multiplying the transformation matrix Ω with the equivariant part of the vector. The transformation matrix Ω may be determined to align the equivariant parts of the vectors of the first set of vectors with the equivariant parts of the respective vectors of the second set of vectors. In some embodiments, the transformation may be a D-dimensional rotation and the transformation matrix Ω may be a D-dimensional rotation matrix. For these embodiments, the transformation matrix Ω may be determined according to the equation:

$$[00006] \Omega = \arg \min_{\hat{\Omega} \in SO(D)} \sum_{i=1}^n \|\hat{\Omega} x_{1,i}^{\text{equiv}} - x_{2,i}^{\text{equiv}}\|^2$$

where $x_{1,i}^{\text{equiv}}$ denotes the equivariant part of vector $x_{1,i}$ and $x_{2,i}^{\text{equiv}}$ denotes the equivariant part of vector $x_{2,i}$. $SO(D)$ denotes the D-dimensional rotation group (i.e. the special orthogonal group of dimension D). The function “arg” in the above equation denotes that the return value is not the minimal value of the sum but the matrix $\{\hat{\Omega}\}$ for which the minimal value of the sum is achieved.

[0157] At **840** the decoder decodes the transformed representation into a reconstructed image (e.g., reconstructed image **480**).

[0158] At **850**, the encoder and the decoder are adjusted (i.e. updated or modified) by adjusting their corresponding sets of encoder and decoder parameters to minimize a loss function (minimize the value of the loss function (pretext loss **142**)). The loss function is based on a metric quantifying a difference between the reconstructed image and the second image. Additionally or alternatively, the loss function may be based on a metric quantifying a difference between the transformed representation and the second representation. By adjusting the encoder and decoder parameters, the pretext machine learning model is adjusted such that it better performs the cross-view alignment task after the adjustment. Adjusting the learnable parameters of the pretext machine learning model (including the parameters of the encoder and the decoder) may be performed by back propagation (e.g. back propagation **144**). After adjusting the pretext machine learning model, the process may stop or repeat. In case that the process repeats, a new iteration is started at **810** with the adjusted pretext machine learning model including the adjusted encoder and decoder. The process may stop after a predetermined number of iterations are complete or when a minimum value of the pretext loss function is reached (e.g., the value of the pretext loss function has converged towards or to a minimum value).

[0159] The two pretext tasks of cross-view completion and cross-view alignment may be combined for training a task specific machine learning model on a downstream geometric vision task. For this purpose, several techniques for combining the methods may be implemented. In a one example (which may be called “early fusion approach”), two separate pretext machine learning models are pre-trained by the training module **50**. The first pretext machine learning model is pre-trained according to the cross-view completion pre-training method **700**. The second pretext machine learning model is pre-trained according to the cross-view alignment pre-training method **800**. This results in two pre-trained encoders, one being pre-trained on the CroCo pretext task and the other being pre-trained on the Caiman pretext task. A task specific machine learning model (e.g., model **170**) for the downstream geometric vision task is constructed by the training module **50** based on or with both of these pre-trained encoders. In one example, supervised fine-tuning (e.g., supervised fine-tuning **150**) is performed by the training module **50** by feeding one or more input images to the first pre-trained encoder resulting in one or more first representations for the one or more input images. Equally, the one or more input images are fed to the second pre-trained encoder by the

training module **50**, which results in one or more second representations for the one or more input images. Subsequently, a joined representation is generated by the training module **50** for each of the one or more input images by concatenating the first and second representations for the respective image. Finally, the joined representations are input in a final task specific layer (e.g., a Multi-layer Perceptron) of the task specific machine learning model. The task specific layer generates task specific output data according to the downstream geometric vision task and a task specific loss (e.g., loss **182**) is determined by the training module **50** based on the output data and the annotated ground truth data of the one or more input images. Finally, the learnable parameters (including the parameters of the encoders and the parameters of the task specific layer) of the task specific machine learning model are adjusted by the training module **50** such as by back propagation (e.g., back propagation **184**).

[0160] In another example, (which may be called “late fusion approach”) for combining cross-view completion pre-training and cross-view alignment pre-training is shown in FIG. **9**, which is a flowchart illustrating a computer-implemented method **900** of generating prediction data for a downstream geometric vision task. Method **900** begins at **910** with training a first task specific machine learning model (e.g., model **170**) for the downstream geometric vision task using cross-view alignment pre-training of a first pretext machine learning model (e.g., model **130**). The training of the first task specific machine learning model is performed according to method **500**, where pre-training step **510** is implemented in accordance with the cross-view alignment pre-training method **800**.

[0161] At **920**, a second task specific machine learning model is trained for the downstream geometric vision task using cross-view completion pre-training of a second pretext machine learning model. The training of the second task specific machine learning model is performed according to method **500**, where pre-training **510** is implemented in accordance with cross-view completion pre-training method **700**. **910** and **920** may be performed sequentially in any order or in parallel.

[0162] At **930** and **940** the two separately trained task specific machine learning models are applied to at least one image to extract respective prediction data from the at least one image. **930** and **940** can be performed sequentially in any order or in parallel. Specifically, first prediction data according to the downstream geometric vision task are generated at **930** by applying the trained first task specific machine learning model to the at least one image. At **940** second prediction data according to the geometric vision task are generated by applying the trained second task specific machine learning model to the at least one image. At **950** a first confidence value is determined for the first prediction data and a second confidence value is determined for the second prediction data. The first confidence value may indicate an expected (e.g., estimated) accuracy of the first predicted data with respect to the downstream geometric vision task. Similarly, the second confidence value may indicate an expected (e.g., estimated) accuracy of the second predicted data with respect to the downstream geometric vision task. The first and second confidence values may be determined by applying the respective trained task specific machine learning model to a test set of annotated images and by comparing the resulting extracted prediction data for the annotated images of the test set to the annotated ground truth data of the annotated images of the test set. As indicated in FIG. **9**, **950** may be performed after **930** and **940** and before **960**. However, **950** may be performed at any point after **910** and **920** and before **960**. In particular, **950** may be performed before **930** and **940** or between these **930** and **940**.

[0163] The method concludes at **960** generating resulting prediction data according to the geometric vision task by fusing the first and second prediction data based on the first and second confidence values. Fusing the first and second prediction data may include determining a weighted sum of the prediction data, where the weights are based on the respective confidence values.

[0164] Although the above examples have been described within the context of methods, they also represent a description of a corresponding component, module, or feature of a corresponding

apparatus or system. Some or all of the method functions may be implemented by a computer in that they are executed by (or using) one or more processors, microprocessors, electronic circuits, and/or processing circuitry.

[0165] The herein-mentioned methods and features may be implemented within an architecture such as illustrated by the functional block diagram of FIG. 10, which includes server **1000** and one or more computing devices (collectively **1002**) that communicate over a network **1004** (which may be wireless and/or wired), such as the Internet, for data exchange. Server **1000** and the computing devices **1002** each include a one or more processors **1012** and memory **1013** such as a hard disk. The computing devices **1002** may include any computing device that communicates with server **1000**, such as an autonomous vehicle **1002b**, robot **1002c**, computer **1002d**, or cell phone **1002e**, or another suitable type of computing device.

[0166] In an example, method **500** of training a task specific machine learning model for a downstream geometric vision task is performed in combination with pre-training methods **600**, **700**, or **800** at server **1000**. The server may provide the trained task specific machine learning model to any of the devices, which may then extract prediction data according to the downstream geometric vision task from one or more images by applying the trained machine learning model to the input one or more images. In an example, one of the devices performs method **500** in combination with pre-training methods **600**, **700**, and **800** to training the task specific machine learning model for the downstream geometric vision task and subsequently applies the trained task specific machine learning model to one or more images to extract prediction data according to the downstream geometric vision task from the one or more images. In various implementations, one of the devices performs method **900** for generating prediction data according to the downstream geometric vision task.

[0167] In a further embodiment, an autonomous apparatus (e.g., vehicle **1002b** or robot **1002c**) may include an optical sensor (e.g., a camera), which generates a first image of the surroundings of the apparatus. The autonomous apparatus may additionally include a second optical sensor (e.g., a second camera), which generates a second image of the surroundings of the apparatus. The first image and the second image depict the surroundings of the apparatus of the apparatus from different viewpoints or from a similar viewpoint at different times. Alternatively, the autonomous apparatus does not include a second optical sensor but stores the second image of the surroundings of the apparatus on a memory device (e.g., memory device **1013b/c**). The stored second image may have been generated by the optical sensor at an earlier time. The autonomous apparatus may train a task specific machine learning model for a downstream geometric vision task according to method **500** in combination with pre-training method **600**, **700**, or **800**. Alternatively, the autonomous apparatus may receive a trained task specific machine learning model from the server, where the server has trained the task specific machine learning model for the downstream geometric vision task according to method **500** in combination with pre-training method **600**, **700**, or **800**. The autonomous apparatus may apply the trained task specific machine learning model to one or more images to extract prediction data from the one or more images according to the geometric vision task. The autonomous apparatus may further adapt its motion state (e.g., velocity or direction of motion) or its operation based on the extracted prediction data. In other words, the autonomous apparatus may adjust its speed and/or steering based on the extracted prediction data.

[0168] In one example the downstream geometric vision task for which the task specific machine learning model has been trained is monocular depth estimation. The autonomous apparatus applies the trained task specific machine learning model to the first image thereby extracting a depth map from the first image, where the depth map corresponds to the surroundings of the autonomous apparatus. The depth map includes a pixel-wise or patch-wise indication of a respective relative distance to a nearest item in the pixel or the patch to the camera taking the image. Based on the extracted depth map, the autonomous apparatus determines a distance to an object in the surroundings of the autonomous apparatus. Based on the determined distance to the object the

autonomous apparatus adjusts its velocity and/or its direction of motion. The autonomous apparatus may adjust its velocity and/or direction of motion, for example, by adjusting power applied to one or more electric motors.

[0169] In another example, the downstream geometric vision task for which the task specific machine learning model has been trained is binocular depth estimation. The autonomous apparatus applies the trained task specific machine learning model to a pair of images thereby extracting a depth map from the pair of images, where the depth map corresponds to the surroundings of the autonomous apparatus. The depth map includes a pixel-wise or patch-wise indication of a respective relative distance of a nearest item in the pixel or the patch to the camera taking the image. The pair of images includes the first image generated by the optical sensor and the second image generated by the second optical sensor, where the images of the image pair are generated by the optical sensors at substantially the same time. Based on the extracted depth map, the autonomous apparatus determines a distance to an object in the surroundings of the autonomous apparatus. Based on the determined distance to the object, the autonomous apparatus adapts its velocity and/or its direction of motion. In other words, the autonomous apparatus may adjust its speed and/or steering based on the extracted distance data.

[0170] In yet another example, the downstream geometric vision task for which the task specific machine learning model has been trained is relative pose estimation. The autonomous apparatus applies the trained task specific machine learning model to a pair of images thereby extracting a relative rotation matrix and a relative translation vector from the pair of images. The pair of images includes the first image generated by the optical sensor and the second image stored at the memory of the apparatus, where the second image has been generated by the optical sensor or another optical sensor at an earlier time than the first image. The memory of the apparatus may additionally store position information of the second image. The position information may indicate a position of the apparatus at the earlier time with respect to the surroundings of the apparatus. Based on the extracted relative rotation matrix, the relative translation vector and the position information, the autonomous apparatus determines a new position of the apparatus with respect to the surroundings of the autonomous apparatus. Based on the determined new position the autonomous apparatus adapts its velocity and/or its direction of motion. In other words, the autonomous apparatus may adjust its speed and/or steering based on the determined position.

[0171] In another example the downstream geometric vision task for which the task specific machine learning model has been trained is optical flow estimation. The autonomous apparatus applies the trained task specific machine learning model to a pair of images thereby extracting pairs of corresponding pixels for the pair of images. The pair of images includes the first image generated by the optical sensor and the second image stored at the memory of the apparatus, where the second image has been generated by the optical sensor at an earlier time than the first image. Each extracted pair of corresponding pixels includes one pixel from the first image and one corresponding pixel from the second image. Based on the extracted pairs of corresponding pixels the autonomous apparatus determines a velocity and/or a direction of motion of an object within the surroundings of the autonomous apparatus. Based on the determined velocity and/or direction of motion of the object, the autonomous apparatus adapts its velocity and/or its direction of motion. In other words, the autonomous apparatus may adjust its speed and/or steering based on the determined speed and/or direction of motion of the object, such as to avoid colliding with the object.

[0172] In yet another example, as described further below, the downstream geometric vision task for which the task specific machine learning model has been trained is depth estimation and visual odometry (including pose estimation). The autonomous apparatus applies the trained task specific machine learning model to a pair of images thereby extracting a depth map and a relative rotation matrix and a relative translation vector from the pair of images. The pair of images includes the first image generated by the optical sensor and the second image stored at the memory of the

apparatus, where the second image has been generated by the optical sensor or another optical sensor at an earlier time than the first image. The memory of the apparatus may additionally store position information of the second image. The position information may indicate a position of the apparatus at the earlier time with respect to the surroundings of the apparatus. Based on the extracted relative rotation matrix, the relative translation vector and the position information, the autonomous apparatus determines a new position of the apparatus with respect to the surroundings of the autonomous apparatus. Based on the determined new position the autonomous apparatus adapts its velocity and/or its direction of motion. In other words, the autonomous apparatus may adjust its speed and/or steering based on the determined position and/or depth map.

[0173] FIG. **11** includes a functional block diagram of an example implementation of the model **130** discussed above for depth and visual odometry. In this example, the model **130** receives images and determines depth maps and poses. The model **130** may also determine a relative translation T between two poses, such as two poses between a pair of input images. The pair of input images may include the same scene and include at least one object that is common to both of the input images. The pair of input images are from two different points of view. The pair of images may be taken at two different times or at the same time from two different cameras at two different locations.

[0174] In various implementations, a control module may actuate one or more actuators of the device based on an output (e.g., depth map, pose, translation) of the model **130**. For example, a control module (e.g., implemented at least in part in memory **1013c**) of the robot **1002c** or a control module (e.g., implemented at least in part in memory **1013b**) of the vehicle **1002b** may steer, accelerate, or decelerate the robot **1002c** or vehicle **1002b**, such as to avoid a human based on an output of the model **130**.

[0175] FIG. **12** includes a functional block diagram of a training system. FIG. **13** includes a functional block diagram of the model **130**.

[0176] A pair of images (denoted I and I' in FIG. **12**) are input to the model **130**. The model **130** includes first and second encoders (modules) **1204** and **1208** corresponding to and function as described above regarding the encoder modules **230**. The first and second encoders **1204** and **1208** encode the images into representations, respectively, as described above.

[0177] The model **130** includes first and second decoders (modules) **1212** and **1216** corresponding to the decoder module **270**. The first and second decoders **1212** and **1216** generate depth maps (D and D') based on the representations output by the first and second encoders **1204** and **1208**, respectively. The depth map D' is for the image I' , and the depth map D is for the image I .

[0178] The model **130** also includes a visual odometry (VO) decoder (module) **1220**. The VO decoder **1220** decodes the representations output by the first and second encoders **1204** and **1208** and generates VO parameters based on the representations. The VO parameters may include, for example, poses of the camera(s) when the images were captured, respectively. The VO parameters may also include a translation T between the images. The poses may be, for example, 6 degree of freedom (DOF) relative poses or another type of pose.

[0179] As illustrated in FIG. **13**, the VO decoder **1220** may include a pose module **1304** and a translation module **1308**. The pose module **1304** decodes the representation output by the encoder **1204** and determines a pose of the camera when the image I' was captured based on the representation output of the encoder **1204**. The pose module **1308** decodes the representation output by the encoder **1208** and determines a pose of the camera when the image I was captured based on the representation output of the encoder **1208**. The translation module **1308** determines a translation T based on a difference between the poses from the pose module **1304**. The translation T may reflect a relative change in position and orientation (e.g., 6 DOF) between the two poses for I and I' .

[0180] A warping module **1224** performs one or more image warping functions and/or determines one or more image warping parameters based on the depth maps, the translation T , and one or more

predetermined camera intrinsic parameters. The predetermined camera intrinsic parameters may include, for example, an indicator if the same camera or camera model was used to capture the images I and I', focal length of the camera(s), shutter speed of the camera(s), aperture of the camera(s), and one or more other intrinsic parameters of the camera(s). As discussed further below, a loss is determined and training is performed to minimize the loss.

[0181] The first and second encoders **1204** and **1208** are trained models as described above for the cross-view completion (CroCo). The first and second decoders **1212** and **1216**, respectively, may be depth decoders and may have a dense prediction transformer (DPT) architecture such as disclosed in U.S. patent application Ser. No. 17/855,763 (published 30 Jun. 2022 as 20230113271) and arXiv publication 2103.13413 entitled "Vision Transformers for Dense Prediction", published 24 Mar. 2021, which are incorporated herein by reference.

[0182] Adapters (modules) **1228** and **1232** are also included with the encoders **1204** and **1208**, respectively. In various implementations, the adapters may be included in the encoders **1204**. The adapters **1128** and **1232** are trained by the training module **50** to learn to minimize the loss.

[0183] To summarize, the encoders **1204** and **1208** are pretrained based on the cross-view completion task using a training dataset. At a finetuning portion of the training, a pair of images (e.g., from two consecutive frames from the same camera) I and I' are input and used to generate the depth maps D and D' respectively and the relative pose translation T between the two images. The loss (e.g., a self-supervised loss L_{self}) is determined (e.g., by a loss module **1312**) which includes a pixel wise depth inconsistency between the depth maps D and D', a geometric consistency loss, and a mask to handle dynamic objects.

[0184] Self-supervised learning/training is a way to learn generalizable visual representations, such as by using different pretext tasks for pretraining. The cross-view completion task is a pretraining task involving training on a large heterogeneous dataset and which enables a network to perceive low-level geometric cues that are relevant to vision downstream tasks. Processed are pairs of images (I, I') which correspond to two different views of the same scene with some overlap. The images may be split into non-overlapping patches. The first input image I may be partially masked, the masked patches are discarded, and the remaining patches are fed to the encoder. The encoder may include the ViT architecture.

[0185] All patches from the second image are encoded using the same encoder with shared weights. The token latent representations output by the encoder from both images are then fed to the decoder that predicts the appearance of hidden patches. The decoder uses a series of transformer decoder blocks including cross-attention layers. This allows non-masked tokens from the first image to attend tokens from the reference image, thus enabling cross-view comparison and reasoning. The model is trained using a pixel reconstruction loss over all masked patches.

[0186] The model **130** as described above includes two branches, one for depth and one for visual odometry, which may share the same encoder. During the finetuning, the training module **50** inputs to the model **130** a pair of images (I, I'), then two decoders process the tokens of both images. For depth, to output a pixel-wise prediction, the ViT layers with a linear MLP head per token may be used in order to generate a dense depth map. The depth decoder may include a series of transformer decoder blocks (e.g., self-attention among token features from the first frame, cross-attention with the token features from the second frame, and an MLP (multi layer perceptron)). The VO decoder may output a 6-DoF relative pose estimation. The VO decoder may include a MLP.

[0187] The DPT may adapt the up convolutions and fusions from multiple layers to vision transformers. This allows features from different blocks to be combined by reshaping them to different resolutions and fusing them with convolutional layers. In practice, the DPT uses the features from four blocks, regularly spread of the decoder depth, starting from the last block. Using transformers in DPT provides more detailed and globally consistent predictions/outputs.

[0188] Regarding the adapters, the adapters are configured to efficiently transfer large pretrained ViT-based models to downstream tasks. The adapters may have the Adaptformer architecture, as

described in Shoufa Chen, et al., Adaptformer: Adapting Vision Transformers for Scalable Visual Recognition, in NeurIPS, 2022, which is incorporated herein in its entirety. The adapters include strong transfer learning abilities by only finetuning a small number of extra parameters.

[0189] FIG. **14** includes an example functional block diagram of an example implementation one layer of one of the encoders **1204** and **1208**. Each layer may be identical, the encoders **1204** and **1208** may be identical in structure, and the adapters may be identical in structure. Each encoder includes N layers, where N is an integer greater than 2. N may be, for example, 8, 12, or another suitable number.

[0190] The layer includes a LayerNorm module **1404** that generates output to a multi-head attention mechanism (module) **1408** using a LayerNorm function. A summer module **1412** adds the output of the multi head attention mechanism **1408** to the input to the LayerNorm module **1404**.

[0191] A LayerNorm module **1416** that generates an output based on an output of the summer module **1412** using a LayerNorm function. A MLP module **1420** generates an output based on the output of the LayerNorm module **1416**. An adapter module **1424** generates an output based on the input to the LayerNorm module **1416**. A summer module **1412** adds the output of the adapter module **1424** to the input to the LayerNorm module **1416**.

[0192] A functional block diagram of the adapter module **1424** is provided on the right in FIG. **14**. A downsizing (downprojection) module **1454** downsizes the input to the LayerNorm module **1416**. A rectified linear unit (ReLU) module **1458** receives the output of the downsizing module **154** and provides output to an upsizing module **1462**. The upsizing module **1462** upsizes the input. A scalar module **1464** scales the output of the upsizing module **1462** using a predetermined scalar and provides the scaled output to the summer **1428**. The right of FIG. **14** illustrates left and right branches.

[0193] Compared to full finetuning, AdaptFormer replaces the MLP block in the transformer encoder with two sub-branches. The MLP layer in the left branch is identical to the original network, while the right branch is an additionally introduced lightweight module for task-specific finetuning. Specifically, the right branch is configured as a bottleneck structure and limits the number of parameters purpose, which includes a down-projection layer (module) with parameters $W_{sub.down} \in \mathbb{R}^{sup.d \times d}$, an up-projection layer (module) $W_{sub.up} \in \mathbb{R}^{sup.d \times d}$, where $\{circumflex over (d)\}$ is a bottleneck middle dimension and satisfies $\{circumflex over (d)\} \ll d$. d may be 768 for the encoders and **512** for decoders or other suitable values. The value of $\{circumflex over (d)\}$ is much smaller (\ll) than d , such as 16 or 32 or another suitable value. FIG. **14** illustrates which portions are trained and which portions are kept frozen.

[0194] During the fine-tuning, the model loads weights from the pretrained model and keeps parameters frozen. The newly added parameters (right branch in FIG. **14**) are updated by the training module **40** on the finetuning data based on minimizing the loss discussed further below.

[0195] Regarding the training, the depth estimation and visual odometry branches are simultaneously finetuned, such as on a predetermined number of monocular videos. Given an adjacent frame pair (I, I') from a training (monocular) video, the depth maps D, D' are generated as described herein, and the relative 6 DOF pose translation is generated as described herein.

[0196] The warping module **1224** may generate a warped depth map $\{circumflex over (D)\}'$ by transforming the depth map D to three dimensional (3D) space using the predetermined camera intrinsics and projecting it to image I' using the pose translation T. The loss module **1312** determines a geometric consistency loss $L_{sub.g}$ based on differences between the warped depth map $\{circumflex over (D)\}'$ and the depth map D' to supervise the training.

[0197] The training module **50** may also generate a warped image \hat{I}' by warping the image I by bi-linear interpolation. The training module **50** may train the adapters based on penalizing color inconsistencies between I and the warped image \hat{I}' . The training module **50** may constrain the geometric consistency between the depth maps D and D' which back propagates the gradients to the adapters.

[0198] The geometric consistency loss L.sub.g aims to force the depth maps D and D' to be as close to each other as possible (consistent with each other in 3D space). The training module **50** may determine the geometric consistency loss L.sub.g using the equation

$$[00007] L_g = \frac{1}{\text{Math. } V \cdot \text{Math.}} \cdot \text{Math. } p \in V D_{diff}(p) \quad (1)$$

where V is a set of valid points successfully projected from I to I' D.sub.diff is the pixel-wise depth inconsistency depth maps D and D',

$$[00008] D(p) = \frac{\text{Math. } \hat{D}(p) - D'(p) \cdot \text{Math.}}{\hat{D}(p) - D'(p)}.$$

[0199] To mitigate the influence of moving objects and occlusions that create geometrical inconsistency across multiple views, the training module **50** may apply a

maskm.sub.S=1-D.sub.diff which assigns lower weights to dynamic objects and occlusions.

[0200] The photometric loss L.sub.p is to force colors to be consistent and not different between I and I'. The photometric loss is configured to constrain the warping between I and I'. The training module **50** may determine the photometric loss using the equation:

$$[00009] L_p = \frac{1}{\text{Math. } V \cdot \text{Math.}} \cdot \text{Math. } p \in V (1 - \lambda) \cdot \text{Math. } I(p) - \hat{I}'(p) \cdot \text{Math. } 1 + \lambda \frac{1 - \text{SSIM}_T(p)}{2} \quad (2)$$

where \hat{I}' is synthesized from I by warping, and SSIM is a metric to measure image structural similarity. λ is a predetermined value, such as approximately 0.85 or another suitable predetermined value. In various implementations, instead of L.sub.p, the training module may determine the photometric loss using a weighted version L.sub.mp, such as using the mask m.sub.s to down-weight regions of moving objects and obstacles, such as using the equation

$$[00010] L_p^m = \frac{1}{\text{Math. } V \cdot \text{Math.}} \cdot \text{Math. } p \in V (m_s(p) \cdot \text{Math. } L_p(p)) \quad (3)$$

[0201] The training module **50** may determine an edge aware smoothness loss L.sub.s to regularize the predicted depth map, such as using the equation:

$$[00011] L_s = \text{Math. } p (e^{-\Delta I(p)} \cdot \text{Math. } \Delta D(p))^2 \quad (4)$$

where Δ is the first derivative along spatial directions, which guides smoothness by image edges. The edge aware smoothness loss is configured to ensure that edges are sharp.

[0202] The loss minimized during the training may be determined based on the above three losses, such as a weighted sum of the losses. For example, the training module **50** may determine the loss and train the adapters based on minimizing the loss, where the loss is determined using the equation:

$$[00012] L_{self} = L_p^m + \beta L_g + \gamma L_s \quad (5)$$

where $\beta=0.5$ and $\gamma=0.1$ or other suitable values.

[0203] The encoders may each include 12 layers and the decoders may use 8 layers in various implementations. In various implementations, four DPT layers may be removed from blocks 2, 4, 6, 8 of the decoder. In various implementations, pixel-wise generation is terminated with 128 heads. In various implementations, the VO decoder may include 2-layer MLP for the 6-DoF pose estimation. Adapters (of dimension $d'=32$, e.g., layers) may be included in both encoder and decoder layers.

[0204] Herein describes training the adapters while freezing the main backbone. The adapters replace the MLP block in the transformer encoder with an AdaptMLP layer, which includes the two sub-branches described above. The MLP layer in the left branch, is frozen, while the right branch introduces a lightweight module for task-specific finetuning.

[0205] The addition of the adapters and the self-supervised fine tuning of the model as discussed herein increases performance for the depth and visual odometry (DVO) task where depth and visual odometry are performed concurrently on a pair of input images. The use of DPT decoders also increases performance. The use of DPT decoders improves depth prediction and makes blurry regions in the depth maps sharper. Adding the adapters increases trainable parameters by a small

amount (e.g., less than 5%) but greatly decreases finetuning time (e.g., by at least 50%).

[0206] FIG. **15** includes an example image and depth maps generated based on the image by other methods (other) and a depth map generated by the model **130** as described herein (present application). As illustrated, the depth map generated by the model **130** has sharper edges and is overall better than the depth maps generated in other ways. In the depth maps, each pixel is given a color where the color indicates the depth (distance between the camera and the object).

[0207] FIG. **16** includes example maps of ground truth (GT) tracks of paths followed by vehicles (e.g., navigating robots) in blue. Each GT position is indicated by a blue dot. FIG. **16** also includes example positions determined by the model **130** in orange as described herein based on images from a camera of the vehicle. Each position determined by the model **130** is indicated by an orange dot. As illustrated, the positions determined by the model **130** closely track the GT positions.

[0208] FIG. **17** includes a flowchart depicting an example method of training the model **130** for concurrent depth estimation and visual odometry. Control begins with **1704** where the training module **50** trains the model as described above based on the cross-view completion (CroCo) task. At **1708**, the training module **50** fine tune trains the adapters **1204** and **1208** as described above using monocular training images that do not have associated annotations based on minimizing the loss $L_{sub.self}$.

[0209] FIG. **18** includes a flowchart depicting an example method of fine tune training the model **130** for concurrent depth and visual odometry. Control begins with **1804** where the training module **50** retrieves a monocular training video (e.g., an i -th video), such as a video that does not have associated annotations regarding depth and poses. At **1808**, the training module **50** may set a counter $T=1$.

[0210] At **1812**, the training module **50** inputs to the model **130** frames T and $T+1$ (the next frame after frame T). The model **50** includes the adapters **1204** and **1208** as discussed above. The model **130** determines the depth maps and pose translation as discussed above based on the pair of images.

[0211] At **1820**, the warping module **1224** performs the warping described above, and the loss module **1312** determines the losses as described above including $L_{sub.self}$. In various implementations, the warping module **112** and the loss module **1312** may be implemented in the training module **50**.

[0212] At **1824**, the training module **50** may determine whether the training video is complete (whether the entire training video has been input to the model **130**). For example, the training module **50** may determine whether $T+1$ is the last frame in the training video. If **1824** is false, the training module may set T equal to $T+1$ at **1828**, and return to **1812** to select input the next two frames/images and of the training video to the model **130**. At the next instance of **1812**, frame $T+1$ from the last instance of **1812** is input to the model **130** as frame T and the next frame (now $T+1$) is also input to the model **130**. If **1824** is true, control may continue with **1832**.

[0213] At **1832**, the training module **50** may determine whether an epoch is complete. For example, the training module **50** may determine whether a predetermined number of training videos have been input to the model **130**. If **1832** is false, the training module **50** may select another monocular training video that does not have associated annotations and begin inputting consecutive frames from that training video to the model **130**. For example, the training module **50** may select the training videos in a random order or in a predetermined order. If **1823** is true, control may continue with **1840**.

[0214] At **1840**, the training module **50** may adjust one or more parameters of one or more of the adapters **1204** or **1208** based on minimizing the loss $L_{sub.self}$ (and thus minimizing each of the losses used to determine the loss $L_{sub.self}$). In various implementations, the training module **50** may instead adjust the parameter(s) of the adapter(s) based on minimizing the loss $L_{sub.self}$ before **1824** and after **1820**. In this way, the adapters **1204** and **1208** would be trained frame pair to frame pair.

[0215] At **1844**, the training module **50** may determine whether the fine tune training is complete. For example, the training module **50** may determine whether a predetermined number of epochs have been completed. If **1844** is true, control may end. If **1844** is false, control may return to **1804** to begin another epoch.

[0216] The foregoing description is merely illustrative in nature and is in no way intended to limit the disclosure, its application, or uses. The broad teachings of the disclosure can be implemented in a variety of forms. Therefore, while this disclosure includes particular examples, the true scope of the disclosure should not be so limited since other modifications will become apparent upon a study of the drawings, the specification, and the following claims. It should be understood that one or more steps within a method may be executed in different order (or concurrently) without altering the principles of the present disclosure. Further, although each of the embodiments is described above as having certain features, any one or more of those features described with respect to any embodiment of the disclosure can be implemented in and/or combined with features of any of the other embodiments, even if that combination is not explicitly described. In other words, the described embodiments are not mutually exclusive, and permutations of one or more embodiments with one another remain within the scope of this disclosure.

[0217] Spatial and functional relationships between elements (for example, between modules, circuit elements, semiconductor layers, etc.) are described using various terms, including “connected,” “engaged,” “coupled,” “adjacent,” “next to,” “on top of,” “above,” “below,” and “disposed.” Unless explicitly described as being “direct,” when a relationship between first and second elements is described in the above disclosure, that relationship can be a direct relationship where no other intervening elements are present between the first and second elements, but can also be an indirect relationship where one or more intervening elements are present (either spatially or functionally) between the first and second elements. As used herein, the phrase at least one of A, B, and C should be construed to mean a logical (A OR B OR C), using a non-exclusive logical OR, and should not be construed to mean “at least one of A, at least one of B, and at least one of C.”

[0218] In the figures, the direction of an arrow, as indicated by the arrowhead, generally demonstrates the flow of information (such as data or instructions) that is of interest to the illustration. For example, when element A and element B exchange a variety of information but information transmitted from element A to element B is relevant to the illustration, the arrow may point from element A to element B. This unidirectional arrow does not imply that no other information is transmitted from element B to element A. Further, for information sent from element A to element B, element B may send requests for, or receipt acknowledgements of, the information to element A.

[0219] In this application, including the definitions below, the term “module” or the term “controller” may be replaced with the term “circuit.” The term “module” may refer to, be part of, or include: an Application Specific Integrated Circuit (ASIC); a digital, analog, or mixed analog/digital discrete circuit; a digital, analog, or mixed analog/digital integrated circuit; a combinational logic circuit; a field programmable gate array (FPGA); a processor circuit (shared, dedicated, or group) that executes code; a memory circuit (shared, dedicated, or group) that stores code executed by the processor circuit; other suitable hardware components that provide the described functionality; or a combination of some or all of the above, such as in a system-on-chip.

[0220] The module may include one or more interface circuits. In some examples, the interface circuits may include wired or wireless interfaces that are connected to a local area network (LAN), the Internet, a wide area network (WAN), or combinations thereof. The functionality of any given module of the present disclosure may be distributed among multiple modules that are connected via interface circuits. For example, multiple modules may allow load balancing. In a further example, a server (also known as remote, or cloud) module may accomplish some functionality on behalf of a module.

[0221] The term code, as used above, may include software, firmware, and/or microcode, and may

refer to programs, routines, functions, classes, data structures, and/or objects. The term shared processor circuit encompasses a single processor circuit that executes some or all code from multiple modules. The term group processor circuit encompasses a processor circuit that, in combination with additional processor circuits, executes some or all code from one or more modules. References to multiple processor circuits encompass multiple processor circuits on discrete dies, multiple processor circuits on a single die, multiple cores of a single processor circuit, multiple threads of a single processor circuit, or a combination of the above. The term shared memory circuit encompasses a single memory circuit that stores some or all code from multiple modules. The term group memory circuit encompasses a memory circuit that, in combination with additional memories, stores some or all code from one or more modules.

[0222] The term memory circuit is a subset of the term computer-readable medium. The term computer-readable medium, as used herein, does not encompass transitory electrical or electromagnetic signals propagating through a medium (such as on a carrier wave); the term computer-readable medium may therefore be considered tangible and non-transitory. Non-limiting examples of a non-transitory, tangible computer-readable medium are nonvolatile memory circuits (such as a flash memory circuit, an erasable programmable read-only memory circuit, or a mask read-only memory circuit), volatile memory circuits (such as a static random access memory circuit or a dynamic random access memory circuit), magnetic storage media (such as an analog or digital magnetic tape or a hard disk drive), and optical storage media (such as a CD, a DVD, or a Blu-ray Disc).

[0223] The apparatuses and methods described in this application may be partially or fully implemented by a special purpose computer created by configuring a general purpose computer to execute one or more particular functions embodied in computer programs. The functional blocks, flowchart components, and other elements described above serve as software specifications, which can be translated into the computer programs by the routine work of a skilled technician or programmer.

[0224] The computer programs include processor-executable instructions that are stored on at least one non-transitory, tangible computer-readable medium. The computer programs may also include or rely on stored data. The computer programs may encompass a basic input/output system (BIOS) that interacts with hardware of the special purpose computer, device drivers that interact with particular devices of the special purpose computer, one or more operating systems, user applications, background services, background applications, etc.

[0225] The computer programs may include: (i) descriptive text to be parsed, such as HTML (hypertext markup language), XML (extensible markup language), or JSON (JavaScript Object Notation) (ii) assembly code, (iii) object code generated from source code by a compiler, (iv) source code for execution by an interpreter, (v) source code for compilation and execution by a just-in-time compiler, etc. As examples only, source code may be written using syntax from languages including C, C++, C#, Objective-C, Swift, Haskell, Go, SQL, R, Lisp, Java®, Fortran, Perl, Pascal, Curl, OCaml, Javascript®, HTML5 (Hypertext Markup Language 5th revision), Ada, ASP (Active Server Pages), PHP (PHP: Hypertext Preprocessor), Scala, Eiffel, Smalltalk, Erlang, Ruby, Flash®, Visual Basic®, Lua, MATLAB, SIMULINK, and Python®.

Claims

1. A non-transitory computer readable medium storing a computer model, the computer model comprising: an encoder module configured to encode first and second images into first and second representations, respectively, the first and second images being from consecutive frames from video; a first decoder module configured to decode the first and second representations and generate first and second depth maps for the images based on the first and second representations, respectively; and a second decoder module configured to determine a six degree of freedom pose

translation of a camera that captured the video based on the first and second representations.

2. The computer model of claim 1 wherein the first and second decoder modules include dense prediction transformer (DPT) decoders.

3. The computer model of claim 1 wherein the encoder module includes adapter modules trained based on minimizing a geometric consistency loss.

4. The computer model of claim 1 wherein the encoder module includes adapter modules trained based on minimizing a photometric loss.

5. The computer model of claim 1 wherein the encoder module includes adapter modules trained based on minimizing an edge smoothness loss.

6. A system comprising: a model including: an encoder module configured to encode first and second images into first and second representations, respectively; a first decoder module configured to decode the first and second representations and generate first and second depth maps for the images based on the first and second representations, respectively; and a second decoder module configured to determine a six degree of freedom pose translation of a camera that captured the video based on the first and second representations; and a training module configured to: train the model using pairs of images, each pair of images including at least part of a same scene and captured at different times; and train parameters of adapter modules of the encoder module using consecutive frames of monocular video based on depth maps and pose translations determined by the model based on the consecutive frames of monocular video.

7. The system of claim 6 wherein the training module is configured to train the parameters of the adapter modules after training the model using the pairs of images.

8. The system of claim 6 wherein the training module is configured to train the parameters of the adapter modules without annotations for the frames of the monocular video.

9. The system of claim 6 wherein the adapter modules include an up projection module, a rectified linear unit (ReLU), and a down projection module, and wherein the training module is configured to train parameters of at least one of the up projection module, the ReLU, and the down projection module based on the depth maps and pose translations determined by the model based on the consecutive frames of monocular video.

10. The system of claim 6 wherein the training module is configured to train the parameters of the adapter modules while all other parameters of the model are fixed.

11. The system of claim 6 wherein the training module is configured to train the parameters of the adapter modules based on minimizing a geometric consistency loss.

12. The system of claim 11 further comprising: a warping module configured to generate a warped depth map based on the first depth map; and a loss module configured to determine the geometric consistency loss based on differences between the warped depth map and the first depth map.

13. The system of claim 12 wherein the warping module is configured to generate the warped depth map further based on the pose translation.

14. The system of claim 13 wherein the warping module is configured to generate the warped depth map based on transforming the first depth map to a three dimensional space and projecting to the second image using the pose translation.

15. The system of claim 6 wherein the training module is configured to train the parameters of the adapter modules based on minimizing a photometric loss.

16. The system of claim 15 further comprising: a warping module configured to generate a warped image based on the first image; and a loss module configured to determine the photometric consistency loss based on differences between the warped image and the first image.

17. The system of claim 16 wherein the loss module is configured to determine the photometric consistency loss based on downweighting regions of the first image including moving objects.

18. The system of claim 6 wherein the training module is configured to train the parameters of the adapter modules based on minimizing an edge smoothness loss.

19. The system of claim 18 further comprising a loss module configured to determine the edge

smoothness loss based on first derivatives of pixel values of the first and second depth maps.

20. The system of claim 6 wherein the first and second decoder modules include dense prediction transformer (DPT) decoders.

21. A method, comprising: train a model using pairs of images, each pair of images including at least part of a same scene and captured at different times, the model including: an encoder module configured to encode first and second images into first and second representations, respectively; a first decoder module configured to decode the first and second representations and generate first and second depth maps for the images based on the first and second representations, respectively; and a second decoder module configured to determine a six degree of freedom pose translation of a camera that captured the video based on the first and second representations; and training parameters of adapter modules of the encoder module using consecutive frames of monocular video based on depth maps and pose translations determined by the model based on the consecutive frames of monocular video.
